UNCLASSIFIED

AD **406 188**

DEFENSE DOCUMENTATION CENTER

FOR

SCIENTIFIC AND TECHNICAL INFORMATION

CAMERON STATION, ALEXANDRIA, VIRGINIA

UNCLASSIFIED

63-3-6

⑤ 625200 ①

NOLTR 62-143
REACTORS - GENERAL

Scale-1

THE STABILITY OF SELECTED
BOUNDARY-LAYER PROFILES

D D C

JUN 19 1963

TISIA A

13 MARCH 1963

NOL

UNITED STATES NAVAL ORDNANCE LABORATORY, WHITE OAK, MARYLAND

NOLTR 62-143

$5.60

(4) 5.60

(5) 625 200

(18) NOLTR (19) $62-143$; ARR 186

Aerodynamics Research Report No. 186

(6) THE STABILITY OF SELECTED BOUNDARY-LAYER PROFILES, $(7-8)$ NA

(9) NA

(10) by

John O. Powers, and Gerhard Heiche and

With Appendix: On the "Dunn-Lin"
Factor in the Secular Equation
for Laminar Stability of Boundary
Layers

by

S. F. Shen

406188

ABSTRACT: An investigation of the stability characteristics of
infinitesimal disturbances in selected laminar boundary-layer
profiles has been conducted. The results of the investigation
give quantitative indications of the influence on boundary-
layer stability of foreign gas injection, applied magnetic
fields, and applied external shear. It is quantitatively shown
that injected gases of large molecular weight and diameter may
result in stabilization, whereas the light, small-diameter gases
are generally destabilizing except for large values of the wall-
to-free-stream temperature ratio. In addition, it is shown that
a moderate external shear yields only percentage changes in the
stability characteristics, whereas an applied magnetic field can
produce order of magnitude changes in the stability.

U. S. NAVAL ORDNANCE LABORATORY
WHITE OAK, MARYLAND

NOLTR 62-143   13 March 1963

The Stability of Selected Boundary-Layer Profiles

                                R. E. ODENING
                                Captain, USN
                                Commander

                                K. R. ENKENHUS
                                By direction

CONTENTS

ILLUSTRATIONS

SYMBOLS

$A(N)$	quantity defined by equation (14)
A_μ	quantity defined by equation (51)
a_ν	coefficients of series in equation (21)
$a_{\mu i}$	coefficients in equation (27) defined by equation (28)
$B(N)$	quantity defined by equation (15)
B_μ	quantity defined by equation (51)
B_0	normal component of magnetic induction
b	magnetic parameter defined by equation (48)
b_i	coefficients in equation (25) defined by equation (26)
b_{ij}	coefficients in equation (31) defined by equation (32)
C	constant in equation (12)
$\bar{C}_p$	constant pressure specific heat of mixture
C_{p_i}	constant pressure specific heat of species "i"
c	dimensionless wave velocity of disturbance
$c_1,\ c_2$	coefficients defined by equation (35)
D	molecular diameter
d_j	coefficient of series in equation (22)
$E(\alpha,c)$	inviscid solution function defined by equation (45)
e_j	coefficient of series in equation (23)
$F(z)$	Tietjens function
$F(w_1)$	concentration function defined by equation (9)
f	mode function for the longitudinal velocity fluctuation
$f(0)$	injection rate parameter defined by equation (46)

$g(u_c)$	function of mode function for transverse velocity fluctuation defined by equation (19)
$g_1(u_c)$, $g_2(u_c)$	first and second independent representations of $g(u_c)$
$g_{1i}(u_c)$, $g_{2i}(u_c)$	series representations of the α^{2i} terms in the series expansions of $g_1(u_c)$ and $g_2(u_c)$ given by equations (29) and (33)
h	dimensionless enthalpy
M_∞	free-stream Mach number
M_1	molecular weight of injected gas
N	transformed normal distance variable
P	quantity defined by equation (13)
Pr	Prandtl number of mixture
Q'	generalized disturbance quantity
q(y)	mode function of generalized disturbance quantity
Re_δ	Reynolds number based on boundary-layer thickness
Re_x	Reynolds number based on length from start of boundary layer
Re_θ	Reynolds number based on boundary-layer momentum thickness
$Re_{\delta*}$	Reynolds number based on boundary-layer displacement thickness
R_i	gas constant for species "i"
r	mode function for the density fluctuation
T	dimensionless temperature
t	dimensionless time
U	dimensional reference velocity
u	dimensionless velocity along surface
u_c	dimensionless velocity difference between u and c
$\bar{u}$	dimensional velocity along surface

$\bar{v}$	dimensional velocity normal to surface
w_1	mass fraction of injected gas
x	dimensionless distance parallel to surface
x_1	mole fraction of injected gas
$\bar{x}$	dimensional distance parallel to surface
Y	quantity defined by equation (45)
y	dimensionless distance normal to surface
$\bar{y}$	dimensional distance normal to surface
z	variable defined by equation (45)
α	dimensionless wave number of the fluctuations
γ	ratio of specific heats in the free stream
δ	dimensional boundary-layer thickness
δ'	dimensional inner viscous layer thickness
Δ	quantity defined by equation (43)
η	Blasius variable, $(y/x)\sqrt{Re_{\bar{x}}}$
θ	mode function for the enthalpy fluctuation
$\bar{\theta}$	dimensional boundary-layer momentum thickness
μ	dimensionless coefficient of viscosity
ν	dimensionless coefficient of kinematic viscosity
ξ	mode function for the concentration fluctuation
$\xi*$	shear parameter defined by equation (47)
τ	mode function for the pressure fluctuation
ρ	dimensionless density
σ	electrical conductivity
ϕ	mode function for the transverse velocity fluctuation
ω	free-stream vorticity

ϖ Schmidt number

Superscripts

'   derivative with respect to the independent variable
            (exceptions are defined above)

(i), (ii), (iii) refers to first, second, or third case as
            defined by equations (39), (40), or (41)

Subscripts

∞ value at infinity

1   refers to injected gas

c   value at critical layer (except for u_c defined above)

m   minimum value of a quantity

N   value of quantity at specific value of N

R, I   real or imaginary part of complex quantity

w   value at the wall

v   viscous quantity

i   inviscid quantity

δ value based on boundary-layer thickness

δ_5 value of quantity when Blasius variable is five

$\delta*$ value based on boundary-layer displacement thickness

θ value based on boundary-layer momentum thickness

The above defined dimensionless quantities are based on a length
scale, δ, (unless otherwise noted by use of a subscript) a time
scale, $\delta/\overline{u}_{\infty}$, and a scale for flow variables corresponding to
their values at the edge of the boundary layer.

INTRODUCTION

The investigation of the stability characteristics of
infinitesimal disturbances in laminar boundary layers has not
produced direct predictions of boundary-layer transition
Reynolds numbers, but it has isolated most of the parameters on
which transition depends as well as indicated their qualitative
effect on transition. The laminar boundary-layer transition
characteristics are of primary importance when aerodynamic
heating and drag considerations predominate vehicle design since
these quantities can increase by an order of magnitude when
boundary-layer flow becomes turbulent. From the standpoint of
aerodynamic heating and possible drag control, considerable
attention has been given in recent years to the techniques of
flow-field control by magnetic fields and by mass transfer.
While these techniques have been shown to be successful for
these purposes in existing laminar or turbulent flows, it is
further important to obtain an indication of the influence of
these techniques with respect to transition from laminar to
turbulent flow. Accordingly, a numerical method based on pro-
cedures outlined by S. F. Shen in reference (1) has been
developed and utilized to investigate the stability of selected
boundary-layer profiles at zero Mach number.

The first group of boundary-layer profiles which demonstrate
the effects of molecular properties of an injected foreign gas
on the laminar boundary layer were obtained from the work leading
to reference (2). While the profiles are not included in
reference (2), several interesting conclusions were deduced from
their analysis. As had been indicated by other investigators,
this analysis demonstrated that injected foreign gases of small
molecular weight were desirable for the reduction of heat trans-
fer. In addition, however, this analysis indicated that, for
low injection rates, an injected foreign gas of large molecular
weight may be more effective in reducing heat transfer than a
small molecular weight gas when a favorable combination of large
molecular diameter and large molar specific heat exists. The
significance of this potential gain could be lost if the larger
molecular weight gas resulted in earlier boundary-layer transi-
tion. Shen, reference (1), has developed an "inviscid criterion"
useful for demonstrating the effect on stability of foreign gas
injection. Application of the "inviscid criterion" shows that
heavy injected gases may tend to be stabilizing, and the present
work allows a more quantitative and complete evaluation of this
tendency.

The second group of boundary-layer profiles was obtained
from the work of E. L. Harris, reference (3). This work is
significant in that recognition has been given to the fact that
flow-field control by magnetic fields may result in magneto-
hydrodynamic layers which are under the influence of an external

1

vorticity induced by the magnetic field. Harris' analysis is
also applicable when there is no magnetic field since vorticity
external to the boundary layer can be induced by a curved shock,
as in the case of the flow near the nose of blunt bodies at
supersonic speed. In this case, the influence of external vorti-
city alone on the boundary-layer stability is of interest. The
stability of magnetohydrodynamic boundary-layer flows without
external vorticity has been adequately* treated by Rossow,
reference (4). Rossow used the approach of Heisenberg as
developed by Lin in reference (5). The numerical approach used
herein is considerably different and, hence, permits comparison
of results obtained by two dissimilar methods.

It is noted that the numerical results presented in the
present report are for incompressible thermal boundary layers,
whereas the procedure of reference (1) and the profiles of
reference (2) are for both incompressible and compressible
boundary layers. The numerical methods used were, in fact,
those for compressible boundary layers and gave good results for
Mach numbers less than 2.2; however, the compressible boundary-
layer profiles of reference (2) were for M = 3.0 and M = 6.0
and, hence, could not be treated by the present method.

ANALYSIS

The present considerations of the boundary-layer stability
analysis are essentially those of reference (1), and only those
portions of the analysis which are necessary for completeness
are repeated here. In some instances additional considerations
are necessary and are clearly indicated as such. The bulk of
the analysis, therefore, deals with the numerical approach used
in obtaining the eigenvalues. As mentioned above, the numerical
procedures are applicable for compressible, as well as incompres-
sible, boundary layers and, hence, all Mach number terms are
retained in the analysis. For the present numerical results
which are for incompressible boundary layers, the Mach number is
simply set equal to zero in all appropriate terms.

LINEARIZED DISTURBANCE EQUATIONS

Foreign gas injection. Only a two-dimensional mean flow
and two-dimensional disturbances have been considered. All
disturbance quantities are assumed of the form:

$$Q' = q(y) e^{i\alpha(x-ct)}$$ (1)

*With the exception noted by J. E. McCune and W. R. Sears, Jour.
of the Aero/Space Sciences, Vol. 26, No. 10, p. 674

where q(y) represents the mode functions, α the wave number and c the wave velocity. Shen, reference (1), using the fact that the viscous effects on fluctuations are considered important only in a layer of thickness δ' where $\delta'/\delta \sim Re_\delta^{-1/2}$,* reduced the linearized equations of motion. Using the disturbance quantities he then arrived at the basic systems of equations, namely:

$$\rho\left[i(u-c)f + \phi u'\right] = -\frac{i}{\gamma M_\infty^2}\pi + \frac{1}{\alpha Re_\delta}\mu f'' \qquad (2)$$

$$\rho\left[i(u-c)\phi\right] = -\frac{1}{\gamma M_\infty^2}\frac{\pi'}{\alpha^2} + \frac{1}{\alpha Re_\delta}\mu \phi'' \qquad (3)$$

$$i(u-c)r + \rho'\phi = -\rho(\phi' + if) \qquad (4)$$

$$\rho\left[i(u-c)\theta + h'\phi\right] = \frac{i(\gamma-1)}{\gamma}(u-c)\pi + \frac{\mu}{\alpha Re_\delta}\cdot$$
$$\left[\frac{\theta''}{Pr} + \frac{1}{\varpi}\left(1 - \frac{\varpi}{Pr}\right)\left(\frac{C_{p_b} - C_{p_a}}{\overline{C_p}}\right)\xi''\right] \qquad (5)$$

$$\rho\left[i(u-c)\xi + w_1'\phi\right] = \frac{1}{\alpha Re_\delta}\frac{\mu}{\varpi}\xi'' \qquad (6)$$

$$\pi = \frac{r}{\rho} + \frac{\theta}{h} + \frac{\xi}{F(w_1)} \qquad (7)$$

where f, ϕ, r, π, θ and ξ are respectively the mode functions for the longitudinal velocity, transverse velocity, density, pressure, enthalpy and concentration fluctuations and by definition:

*This ordering as of Dunn and Lin, reference (6), is considered adequate for low Mach numbers. Reshotko, reference (7), has pointed out that refinements in ordering might be desirable at higher Mach numbers. Such refinements should not affect the low Mach number trends.

$$\overline{Cp} = Cp_a + W_1\left(Cp_b - Cp_a\right) \tag{8}$$

$$\frac{1}{F(w_1)} = \frac{R_b - R_a}{R_b + W_1(R_b - R_a)} - \frac{Cp_b - Cp_a}{Cp_a + W_1\left(Cp_b - Cp_a\right)} \tag{9}$$

Shear and Magnetohydrodynamics. For small external shear the basic equations of the stability problem are unaltered, and the influence of the shear enters only through the outer boundary conditions. Hence, the disturbance equations are unchanged, and the two-dimensional mean flow with external shear presents no additional complications since the dominating boundary condition d^2u/dy^2 equal to zero for $y = \infty$ is retained. The magneto-hydrodynamic profiles, however, require detailed consideration which, for the case treated herein of transverse magnetic fields, has been given by Lock, reference (8). In reference (8), after the derivation of the linearized small disturbance equations, an assumption that the Reynolds number was not too large ($R_\delta < 10^5$) permitted Lock to demonstrate an analogy of Squire's theorem and also to develop a magnetohydrodynamic Orr-Sommerfeld equation. This equation differed from the ordinary Orr-Sommerfeld equation in one term which was shown to be negligible and which also vanishes in the conventional separation to the "inviscid" and "viscous" equations. The effect of the transverse magnetic field on the stability analysis, therefore, appears only in the manner in which the magnetic field alters the mean-flow profile. While, as a result of the δ' ordering, equations (2) through (7) do not reduce directly to the Orr-Sommerfeld equation for zero Mach number and zero foreign gas injection, they do yield under these conditions the same "inviscid" and "viscous" equations and, hence, we need consider further only one set of disturbance equations for all profiles considered herein.

METHOD OF SOLUTION

The general method of solution of the system of equations (2) through (7) is conventional in that separate "inviscid" and "viscous" solutions are obtained and the combination of these solutions satisfying the boundary conditions leads to the eigen-value relation. The "inviscid equation" which is derived for large Re_δ is integrated numerically from the edge of the boundary layer to the neighborhood of the "critical layer" (i.e. where $u = c$, see equation (15)). At the "critical layer" singularity, in a manner somewhat similar to the method employed by Timman, et al., reference (9), the solution was continued past the

4

singularity by a power series representation. The present
expansion differs from that of reference (9) since they used
an expansion in the normal distance variable, whereas an
expansion in both (u-c) and α^2 is used in the present method.
After the critical layer the inviscid solution becomes complex,
and both real and imaginary parts are integrated numerically
until their values at the wall are obtained. At the wall the
viscous solutions which are obtained from an asymptotic series
in $\left(\alpha \, Re_\delta\right)^{-\frac{1}{2}}$ are joined through the boundary conditions with
the inviscid solutions; and the eigenvalues, α and Re, are
obtained for a given value of c_R (i.e. with $c_I = 0$). Hence, a
point on the neutral stability curve for the boundary layer
profile under investigation is obtained.

The Inviscid Equation. The "inviscid equation" for the
transverse velocity fluctuations may be found directly from
equations (2) through (7) by letting $Re_\delta \rightarrow \infty$ and on proper
combination may be shown to be:

$$\frac{d}{dy}\left[\frac{(u-c)\phi'-u'\phi}{\frac{1}{\rho}-M_\infty^2(u-c)^2\left(\gamma-\frac{\gamma-1}{\rho h}\right)}\right]-\alpha^2\rho(u-c)\phi=0 \qquad (10)$$

When the Mach number is set equal to zero this reduces to:

$$\frac{d}{dy}\left\{\rho\left[(u-c)\phi'-u'\phi\right]\right\}-\alpha^2\rho(u-c)\phi=0 \qquad (11)$$

where it is seen that the influence of foreign gas injection is
manifested through the density of the mixture as well as through
the effect of the injection on the form of the velocity profiles.
As might be expected for the constant density shear and magneto-
hydrodynamic profiles the stability is determined completely by
the form of the velocity profile.

For the numerical solution of equation (10) it is expedient
to change independent variables and introduce certain notational
simplifications. The new independent variable is obtained by
using the Dorodnitsyn transformation, the Blasius variable, and
changing the sign of the coordinate normal to the flow. The
first two changes are conventional, and the last change is simply
introduced because equation (10) is integrated from the edge of
the boundary layer to the wall. The resulting new variable, N,

5

is, therefore, defined by:

$$CdN = -\rho d\eta = -\frac{\rho dy}{X}\sqrt{Re_{\overline{x}}}$$ (12)

where the value $N = 1$ was chosen for the outer edge of the boundary layer.

We next define:

$$P(N) = \frac{1}{\rho^2} - M_{\infty}^2 u_c^2 \left(\frac{\gamma}{\rho} - \frac{\gamma-1}{\rho^2 h}\right)$$ (13)*

$$A(N) = \frac{1}{P}\frac{dP}{dN}$$ (14)

$$B(N) = \frac{1}{u_c}\left(\frac{d^2 u}{dN^2} - A\frac{du}{dN}\right) + \alpha^2 P$$ (15)

where $u_c = u-c$, and α has been non-dimensionalized by δ which is, in turn, defined up to a constant as $\delta = $ constant $\frac{x}{\sqrt{Re_{\overline{x}}}}$. It is now possible to rewrite equation (10) as:

$$\frac{d^2\phi}{dN^2} - A(N)\frac{d\phi}{dN} - B(N)\phi = 0$$ (16)

The outer boundary condition for equation (16) is found from the relation:

$$\frac{d^2\phi}{dN^2} - \left[\frac{1}{P}\frac{dP}{dN}\right]\frac{d\phi}{dN} - \left[\alpha^2 P - \frac{1}{Pu_c}\frac{du}{dN}\frac{dP}{dN}\right]\phi = 0$$ (17)

which is evaluated at the outer edge of the boundary layer, i.e. at $N = 1$. (Note that from equation (12) N increases as the wall is approached.) For the shear profiles with $M_{\infty} = 0$, $dP/dN = 0$ at $N = 1$, but for the injection profiles, both $\frac{dP}{dN}$ and $\frac{du}{dN}$ are

equal to zero at $N = 1$. This gives from equation (17)

*Note: This definition of P differs from that of reference (1), equation (25) by a factor of $1/\rho$.

6

$$\frac{1}{\phi}\frac{d\phi}{dN} = \propto P^{\frac{1}{2}}$$ (18)

as the condition for bounded disturbances at large distances from the wall (i.e. as $N \rightarrow -\infty$) since P is restricted to positive values and is considered constant at its value for N = 1. It is observed that for the shear profiles with Mach numbers not equal to zero the conditions necessary for equation (18) would not be realized, but this case has not been treated herein. In the present numerical procedure, equation (18) and normalization of ϕ at N = 1 were the conditions used to start the numerical integration.

Expansion Around the Critical Layer. In order to continue the solution of the inviscid equation in the neighborhood of the critical layer, i.e. where u = c and where a logarithmic singularity exists, a local power series representation was used. For the power series representation the independent variable u_c = u-c was utilized, and the mode function $\phi(N)$ was replaced by the variable $g(u_c)$ according to the definition:

$$\phi(N) = U_c\, g(U_c)$$ (19)

These relations may be used to transform equation (16) into the following second order linear differential equation:

$$\frac{d^2 g}{du_c^2} + \left[\frac{2}{U_c} + \frac{d^2 u}{dN^2} \bigg/ \left(\frac{du}{dN}\right)^2 - A(N) \bigg/ \frac{du}{dN}\right]\frac{dg}{du_c} - \left[\propto^2 P(N) \bigg/ \left(\frac{du}{dN}\right)^2\right] g = 0$$ (20)

Equation (20) has two independent solutions, $g_1(u_c)$ and $g_2(u_c)$, which are represented as two power series. The first solution is written in the form:

$$g_1(U_c) = \sum_{\nu=0}^{\infty} a_\nu\, U_c^\nu$$ (21)

and then it is necessary to determine the coefficients a_ν. It can be assumed that a_0 = 1. To obtain the further coefficients, a_ν, the coefficients in equation (20) were developed in power series:

$$\frac{d^2 u}{dN^2} \bigg/ \left(\frac{du}{dN}\right)^2 - A(N) \bigg/ \frac{du}{dN} = \sum_{j=1}^{\infty} d_j\, U_c^{j-1}$$ (22)

7

$$P(N) \Big/ \left(\frac{du}{dN}\right)^2 = \sum_{j=1}^{\infty} e_j u_c^{j-1} \tag{23}$$

Later, for the actual numerical calculations, terms higher than u_c^4 were neglected. Insertion of equations (21), (22), and (23) into (20) and grouping of like powers of u_c yield the following expressions for the coefficients, a_ν

$$a_0 = 1 \qquad a_1 = 0 \qquad a_2 = \propto \frac{e_1}{6}$$

$$a_\mu = \frac{1}{\mu(\mu+1)} \left[-\sum_{\ell=1}^{\mu-1} d_{\mu-\ell} \, \ell a_\ell + \propto^2 \sum_{\ell=0}^{\mu-2} e_{\mu-\ell-1} \, a_\ell \right] \quad \mu \geq 3 \tag{24}$$

A second independent solution, $g_2(u_c)$, of equation (20) is found by the method of variation of parameters utilizing equations (21) and (24). This solution is

$$g_2(u_c) = d_1 g_1(u_c) \ln u_c + \frac{1}{u_c} + \sum_{i=1}^{\infty} b_i u_c^i \tag{25}$$

Proceeding as before, equations (22), (23), and (29) are put in (20) and the following expression for the b_i's is obtained:

$$b_i = \frac{1}{i(i+1)} \left[d_{i+1} - d_1 d_i - (2i+1) a_i d_1 - \sum_{j=1}^{i-2} d_1 d_j a_{i-j} \right.$$
$$\left. - \sum_{j=1}^{i-1} j \, d_{i-j} b_j + \propto^2 \left(e_i + \sum_{j=1}^{i-2} e_{i-j-1} b_j \right) \right] \tag{26}$$

It is noted from (22) and (23) that d_j and e_j depend on the particular profile and the value of c. From (24) and (26) it is apparent that a_μ and b_i depend, furthermore, on the value of a^2. In order to conserve machine time for the actual calculation, the a_μ and b_i were next expanded in terms of a^2:

$$a_\mu = a_{\mu 0} + a_{\mu 2} \propto^2 + a_{\mu 4} \propto^4 + a_{\mu 6} \propto^6 + \ldots \tag{27}$$

and using equation (24) we get, therefore:

8

$$a_{00} = 1 \qquad a_{\mu 0} = 0 \qquad \text{for } \mu \geq 1$$

$$a_{02} = a_{12} = 0 \qquad a_{\mu 2} = \frac{1}{\mu(\mu+1)}\left[e_{\mu-1} - \sum_{\ell=2}^{\mu-1} \ell d_{\mu\ell}\, a_{\mu 2}\right] \mu \geq 2$$

$$a_{04} = a_{14} = a_{24} = a_{34} = 0$$

$$a_{\mu 4} = \frac{1}{\mu(\mu+1)}\left[\sum_{\ell=2}^{\mu-2} e_{\mu-\ell-1}\, a_{\mu 2} - \sum_{\ell=4}^{\mu-1} \ell d_{\mu-\ell}\, a_{\ell 4}\right] \mu \geq 4 \qquad (28)$$

$$a_{06} = a_{16} = a_{26} = a_{36} = a_{46} = a_{56} = 0$$

$$a_{\mu 6} = \frac{1}{\mu(\mu+1)}\left[\sum_{\ell=4}^{\mu-2} e_{\mu-\ell-1}\, a_{\mu 4} - \sum_{\ell=6}^{\mu-1} \ell d_{\mu-\ell}\, a_{\ell 6}\right] \mu \geq 6$$

The value of μ in equation (28) was limited to six and, hence, equation (21) may be written as:

$$g_1(u_c) = 1 + \alpha^2 g_{11}(u_c) + \alpha^4 g_{12}(u_c) + \alpha^6 g_{13}(u_c) \qquad (29)$$

where

$$g_{11}(u_c) = a_{22} u_c^2 + a_{32} u_c^3 + a_{42} u_c^4 + a_{52} u_c^5 + a_{62} u_c^6$$

$$g_{12}(u_c) = a_{44} u_c^4 + a_{54} u_c^5 + a_{64} u_c^6 \qquad (30)$$

$$g_{13}(u_c) = a_{66} u_c^6$$

As with the a_μ's, this equation may be written in powers of α^2 in the form:

$$b_i = b_{i0} + b_{i2} \alpha^2 + b_{i4} \alpha^4 + \ldots \qquad (31)$$

9

where higher order terms than α^4 are negligibly small when compared with terms like $1/u_c$. From equations (26) and (31), one may obtain:

$$b_{i0} = \frac{1}{i(i+1)}\left[d_{i+1} - d_1 d_i - \sum_{j=1}^{i-1} j\, d_{i-j}\, b_{j0}\right]$$

$$b_{i2} = \frac{1}{i(i+1)}\left[e_i - (2i+1)a_{i2}d_1 - \sum_{j=1}^{i-2} a_{(i-j)2}d_1 d_j - \sum_{j=1}^{i-1} j\, b_{j2}\, d_{i-j} + \sum_{j=1}^{i-2} b_{j0}\, e_{i-j-1}\right] \tag{32}$$

$$b_{i4} = \frac{1}{i(i+1)}\left[-(2i+1)a_{i4}d_1 - \sum_{j=1}^{i-2} a_{j4}d_1 d_j - \sum_{j=1}^{i-1} j\, b_{j4}\, d_{i-j} + \sum_{j=1}^{i-2} b_{i2}\, e_{i-j-1}\right]$$

Paralleling the form of equation (29), the following expression is written for g_2:

$$g_2(u_c) = d_1 g_1(u_c)\, \ell n\,|u_c| + g_{20}(u_c) + \alpha^2 g_{21}(u_c) + \alpha^4 g_{22}(u_c) \tag{33}$$

where:

$$g_{20}(u_c) = \frac{1}{u_c} + b_{10} u_c + b_{20} u_c^2 + b_{30} u_c^3 + b_{40} u_c^4$$

$$g_{21}(u_c) = b_{12} u_c + b_{22} u_c^2 + b_{32} u_c^3 + b_{42} u_c^4 \tag{34}$$

$$g_{22}(u_c) = b_{34} u_c^3 + b_{44} u_c^4$$

The general solution $g(u_c)$ of equation (20) is a linear combination of $g_1(u_c)$ and $g_2(u_c)$, namely:

$$g(u_c) = c_1 g_1(u_c) + c_2 g_2(u_c) \tag{35}$$

which in turn from equation (19) yields:

$$\phi(N) = u_c\left[c_1 g_1(u_c) + c_2 g_2(u_c)\right] \tag{36}$$

The coefficients c_1 and c_2 are determined at some small value of u_c (i.e. $1 \gg u_c > 0$) by equating $\phi(N)$ and $\frac{d\phi}{dN}$ from equation (36) to their corresponding values from the numerical integration of equation (16), which is discussed in the second paragraph on page 14. With these coefficients known, we proceed around the

singularity to a negative u_c whose absolute value is approximately equal to the positive value of u_c used in determining the coefficients. On this side of the singularity the solution, equation (36), becomes complex as is discussed by Lin in reference (10). Accordingly, it may be written as:

$$\phi = \phi_R + i \phi_I \qquad (37)$$

where: $\phi_R = u_c \, g(u_c)$

and for $u_c < 0$: $\qquad\qquad\qquad\qquad\qquad\qquad (38)$

$$\phi_I = -c_2 \, d_1 \, \pi \, u_c \, g_1(u_c)$$

We now note that the coefficients $A(N)$ and $B(N)$ of equation (16) are real and, therefore, the differential equation may be integrated separately for ϕ_R and ϕ_I in the manner discussed in the paragraph on numerical procedures. This is done for values of N from just below the critical layer to the wall yielding the values of ϕ_{R_w} and ϕ_{I_w} (where the subscript w indicates wall values), which are to be used in the eigenvalue problem. In addition to the above discussed "critical layer" singularity, an "apparent" singularity occurs when P equals zero in equation (14). From equation (13) it is seen that this occurs when $M\infty^2 = \left[\rho u_c^2 \left(\delta - \frac{\delta-1}{\rho h}\right)\right]^{-1}$. This takes place when the local relative velocity of the disturbance becomes sonic. This was found to occur at Mach numbers somewhat greater than 2. The "apparent singularity" can be avoided by a change of dependent variables as is shown in reference (11); however, even then the coefficients of the resulting differential equation change sign. In the present case, $A(N)$ (see equation (14)) changes sign when P changes sign and the Sturm-Lionville theorem can no longer be applied to guarantee the existence of eigensolutions of the differential equation (16). The full significance of the "apparent singularity" has not as yet been explored. The fact that Brown, reference (12), has obtained reasonable solutions at a Mach number of 5.8 by a direct integration of the ordered disturbance equations obviously indicates that numerical procedures can give realistic results at high Mach numbers, but the possibility of obtaining physically reasonable results by a matching of viscid and inviscid solutions remains to be demonstrated.

The Viscous Solutions and the Eigenvalue Problem. The developments of the viscous solutions are given in detail in references (1) and (11) and also Appendix A (Some of the equations of reference (1) have been revised by Shen who has suggested that the improved relations be included as Appendix A to the present report.). An informative discussion of viscous solutions is given in reference (13). Here we only briefly outline the development associated with the present numerical procedure which is essentially that of reference (1) and Appendix A.

The equations (2) through (7) are written as a system of first order differential equations and, following a method suggested by Tollmien, a solution by asymptotic series is attempted which yields improved viscous solutions valid at large distances from, as well as near to, the critical layer. Using the asymptotic expansions, three sets of zeroth order solutions were obtained:

(i) $\qquad$ (39)

$$f_v \approx \exp\left\{\sqrt{\alpha R_{e\delta}}\int_{y_c}^{y}\left(-\sqrt{i\frac{(u-c)}{\nu}}\right)dy\right\};\ \phi_v = \frac{\pi v}{M_\infty^2} = \theta_v = \xi_v = 0$$

(ii) $\qquad$ (40)

$$\theta_v \approx \exp\left\{\sqrt{\alpha R_{e\delta}}\int_{y_c}^{y}\left(-\sqrt{iP_r\left(\frac{u-c}{\nu}\right)}\right)dy\right\};\ f_v = \phi_v = \frac{\pi v}{M_\infty^2} = \xi_v = 0$$

(iii) $\qquad$ (41)

$$\left.\begin{array}{c}\xi_v\\\phi_v\end{array}\right\}\approx \exp\left\{\sqrt{\alpha R_{e\delta}}\int_{y_c}^{y}\left(-\sqrt{i\varpi\left(\frac{u-c}{\nu}\right)}\right)dy\right\};\ f_v = \frac{\pi v}{M_\infty^2} = \theta_v = 0$$

For high-frequency fluctuations the boundary conditions at the wall are: $f(0) = \phi(0) = \theta(0) = \xi(0) = 0$; then by referring to the orders of magnitude of the asymptotic solution, Shen, reference (1), derived the secular equation as:

$$\frac{\phi_i(0)}{f_i(0)} = \frac{\phi_v^{(i)}(0)}{f_v^{(i)}(0)}(1+\Delta)$$ (42)

where:

$$\Delta = \frac{\phi_v^{(ii)}(0)f_v^{(i)}(0)}{\phi_v^{(i)}(0)f_i(0)}\left[\frac{\theta_i(0)}{\theta_v^{(ii)}(0)} + \frac{\xi_i(0)}{\xi_v^{(iii)}(0)}\left(\frac{\phi_v^{(iii)}(0)}{\phi_v^{(ii)}(0)} - \frac{\theta_v^{(iii)}(0)}{\theta_v^{(ii)}(0)}\right)\right] + O\left(1/\sqrt{\alpha R_{e\delta}}\right)$$

$$f_i(0) = \left\{\frac{i}{\rho P}\left[\frac{1}{\rho}\phi' - M_\infty^2 u' u_c\left(\gamma - \frac{\gamma-1}{\rho h}\right)\phi\right]\right\}_w$$ (43)

In (42) the superscripts refer to the cases (i), (ii), or (iii) for which the zeroth order solutions are given by equations (39) through (41).

Equation (42) is similar to the secular relation given by Dunn and Lin in reference (6). In fact, when the concentration fluctuations are not present, it is exactly the secular relation of reference (6). Dunn and Lin show Δ to be directly proportional to the square of the Mach number and, hence, for the present Mach number zero profiles, Δ was also set equal to zero since only small injection rates are considered. A comparison of solutions at a Mach number of 1.3, figure 1, by the present method which neglects Δ and the method of reference (13) which effectively contains Δ shows very good agreement. Hence, as Mack pointed out, the temperature fluctuations apparently have no effect on the neutral stability curve at this Mach number. Accordingly, no effect of temperature fluctuations is expected at lower Mach numbers. Further, it is felt for the case of small injection that the contribution of the concentration fluctuations to the correction factor Δ should not be large enough to obscure any of the indicated trends. Using Dunn and Lin's improvement on the viscous solutions and retaining our independent variable, N, we may rewrite equation (42) as:

$$ E(\alpha, C) = F(Z) \tag{44} $$

where:

$$ E(\alpha, C) = \frac{\phi(N_w)}{f(N_w)} \frac{1}{Y} $$

$$ Y = \frac{3}{2} \left(\frac{\nu_w}{C}\right)^{\frac{1}{2}} \int_{N_C}^{N_w} \frac{\sqrt{-U_c/\nu}}{\rho} \, dN \tag{45} $$

$$ Z = (\alpha R_{e\delta})^{\frac{1}{3}} \left[-Y\right]^{\frac{2}{3}} $$

and F(z) represents the well-known "Tietjens Function." For the present numerical calculations, the "Tietjens Function" of reference (14) was used. The eigenvalues are obtained from equation (44), and equations (45) are used to compute the corresponding Reynolds numbers.

Numerical Procedures. The profiles used were given in the form of discrete points. Numerical procedures, therefore, had to be selected for interpolation, differentiation, and integration. The schemes were selected such that the results of these operations differed from known results by a minimal amount

13

when compared with respect to the sum of the least square devia-
tion. The basis for this comparison was the Blasius profile,
since the complete profile and its derivatives are known.

From equation (15) it is apparent that the "inviscid"
equation (16) has a singularity at u = c. As indicated in the
discussion of the general method of solution, page 4, the
inviscid equation was integrated numerically for the entire
range of the independent variable except in a small neighborhood
of this singularity. The integration procedure, which uses the
fourth order Adam Moulton predictor-corrector method with the
Runge Kutta method for starting and stopping, is described in
reference (15). In order to be able to choose freely the step
size of integration, the coefficients A(N) and B(N) of equation
(16) were interpolated directly. This direct interpolation of
the final coefficients is more accurate than using interpolated
profile values in the calculation of these coefficients. By
integrating with different step sizes, it was found that the
values of the transverse velocity fluctuation mode functions, ϕ,
were not changed by making the step size smaller than 1/500 of
the boundary-layer thickness, δ.

The results are even more sensitive to the closeness of
approach to the critical point, u = c. If we integrate numeri-
cally too close to the singularity, the rapid growth of the coef-
ficient B(N) in equation (16) affects the result. If, on the
other hand, we stay too far away from the singularity, accuracy
is lost in "the going around the singularity" by power series
because the actual calculation had to be performed with poly-
nomials of finite degree. The best compromise was to choose the
critical distance between 1/50 to 1/100 of the boundary-layer
thickness, δ.

Finally, an overall check for the accuracy of the results
was given by comparison with already known stability curves,
such as for the Blasius profile (See fig. 7 and first paragraph
of Results and Discussion) or the Mach 1.3 case (See fig. 1).

BOUNDARY-LAYER PROFILE DATA

Foreign Gas Injection. The boundary-layer profile data
which included the injection of a foreign gas were taken from
the work of I. Korobkin, reference (2). By assuming that the
blowing velocity varies inversely with the square root of the
distance from the leading edge, he was able to obtain similar
profiles. This, in turn, implies concentration profiles
independent of x which, when coupled with the condition of zero
net flux of the free-stream component across the wall, deter-
mined the wall concentration, $w_1 = \rho_1/\rho_\infty$, for a given value of
the injection rate parameter:

$$f(0) = -2 \frac{\rho_w \overline{V_w}}{\rho_\infty U_\infty} \sqrt{Re_{\overline{x}}} \qquad (46)$$

14

All calculations were made for a value of the injection rate parameter of one-tenth.

In reference (2), boundary-layer profiles were computed for twenty-seven gases by making all possible combinations of the molecular weights, molecular diameters, and specific heats of He, air, and CCl_4. In the present work, we have dealt with the three real gases, He, air, and CCl_4, and have not considered any of the possible hypothetical combinations. The boundary-layer profiles for zero blowing, air injection, helium injection, and carbon tetrachloride injection are presented, respectively, in figures 2, 3, 4, and 5. These profiles, which have not been given previously, are given for wall-to-stream temperature ratios of 0.5, 1.0, and 2.0. For these profiles the boundary-layer thickness, δ, was taken as corresponding to N - 1, since this was the thickness used for the calculations of the reference (2) profiles. This is equivalent to using boundary-layer thicknesses in terms of the Blasius variable ranging from nine to thirteen. The effect on comparative stability results for profiles having thicknesses in this range is negligible as is demonstrated in the first two paragraphs of the section on Results and Discussion.

Shear and Magnetohydrodynamic Profiles. The boundary-layer profiles giving the first order effects of external shear, applied transverse magnetic fields, and a combination of these effects were taken from the work of E. L. Harris, reference (3). He assumed that a perturbation expansion of the stream function was possible for small values of the shear parameter, ξ^*, and magnetic parameter, b.

$$\xi^* = \omega \bar{x} / U_\infty \sqrt{Re_{\bar{x}}} \qquad (47)$$

$$b = \sigma B_o^2 \bar{x} / \rho U_\infty \qquad (48)$$

where:

ω = free-stream vorticity

B_o = normal component of the magnetic induction

σ = electrical conductivity

Using such an expansion the resulting system of differential equations could be treated in a manner which readily permitted independent analysis of the free-stream vorticity and magnetic field effects. The profiles used in the present investigation, figure 6, were for magnetic and shear parameters of one-tenth (i.e. $\xi^* = 0.1$ and b = 0.1). In the stability analysis an arbitrary value was assigned to the outer edge of the shear

profiles so that a value of the free-stream velocity could be
determined for a non-dimensionalizing reference. For this
purpose the value of the Blasius variable of five was used.
With respect to the definition of the momentum thickness, $\bar{\theta}$, it
was herein considered that the free-stream velocity to be used
in the calculations should be the flow velocity used to normalize
the velocity at η equal to five. When the boundary-layer equa-
tion of motion for zero pressure gradient, reference (3), is
integrated with respect to y for a shear flow, the usual integral
momentum equation is not obtained because the x component of the
velocity increases continuously with y. This variation of the
velocity leads to an ambiguity in the expression for the momentum
thickness. Therefore, since the value of the momentum thickness
could actually be considered to vary with the choice of δ, we
have for convenience defined a pseudo momentum thickness as:

$$\bar{\theta} = \int_0^{\bar{y}_{\delta 5}} \left[\frac{\bar{\rho}\bar{u}}{\bar{\rho}_\infty U_{\delta 5}} \left(1 - \frac{\bar{u}}{U_{\delta 5}} \right) \right] d\bar{y} \qquad (49)$$

where $U_{\delta 5}$ is the value of the velocity when the Blasius variable
is five. To provide a more meaningful basis for comparison,
the minimum critical Reynolds numbers of these profiles are
presented also as length Reynolds numbers.

TRANSPORT PROPERTIES

While all transport properties are important in the compu-
tation of the boundary-layer mean flow profiles, the most impor-
tant transport property in the stability analysis as formulated
herein is the viscosity. This is apparent when one examines
equations (45) and observes that through the quantity Y the
viscosity can influence the eigenvalues and in combination with
z can affect the value of the corresponding Reynolds number.
To obtain a reasonable value for the viscosity of the air-
injected foreign gas mixture, the formula (8.2-22) of reference
(16) was used. The fact that the viscosity of the mixture is
used in ratio to the free-stream viscosity leads to ratios of
the collision integrals as functions of the reduced temperatures.
Considering the maximum attractive energy between molecules of
the kind used herein, as well as the dependency of the collision
integrals on the maximum attractive energies, and in view of the
compensating manner in which the ratios of the integrals enter
the viscosity relation, it becomes reasonable to set the ratio
of the collision integrals equal to unity. This assumption
permits us to express formula (8.2-22) of reference (16) in the
following somewhat simplified form:

$$\mu = \sqrt{T}\, \frac{A_\mu}{B_\mu} \qquad (50)$$

16

where:

$$A_\mu = 1 + 0.6 \left\{ \frac{X_1^2 M_1}{29} + 2X_1(1-X_1)\left[\frac{1}{4}\left(\frac{M_1}{29} + 2 + \frac{29}{M_1}\right)\left(\frac{\sqrt{\frac{32}{\frac{M_1}{29}} + 1}}{\left(1 + \frac{3.65}{D}\right)^2}\right) \right. \right.$$

$$\left. \left. + \frac{\sqrt{\frac{32}{\frac{29}{M_1}} + 1}}{\left(1 + \frac{D}{3.65}\right)^2}\right) - 1\right] + \left(1 - X_1\right)^2 \frac{29}{M_1} \right\}$$

$$B_\mu = X_1^2 \left(\frac{D}{3.65}\right)^2 \left(1 + 0.6\frac{M_1}{29}\right)\sqrt{\frac{29}{M_1}} + 2X_1(1-X_1)\left[\left(1 + \frac{D}{3.65}\right)^2 \cdot \right.$$

$$\left. \sqrt{\frac{1 + \frac{29}{M_1}}{32}} + 0.15 \frac{\left(\frac{M_1}{29} + 2 + \frac{29}{M_1}\right)\sqrt{\frac{32}{\frac{M_1}{29}} + 1}}{\left(1 + \frac{3.65}{D}\right)^2}\right] + \left(1 - X_1\right)^2\left(1 + 0.6\frac{29}{M_1}\right)$$

(51)

$$X_1 = \frac{W_1}{W_1 + (1-W_1)\frac{M_1}{29}}$$ = mole fraction of injected gas

$$W_1 = \rho_1 / \rho$$ = mass fraction of injected gas

M_1 = molecular weight of injected gas (4, 29, or 154 for He, air, or CCl_4)

D = molecular diameter in Angstroms (2.6, 3.65, or 5.88 for He, air, or CCl_4)

In equation (51) it is noted that most of the numerical constants correspond to the air values. This occurs because the value of the viscosity at the edge of the boundary layer (i.e. the value for the free-stream air) is used as the scale for the viscosity flow variable. Equation (50) was used in all of the numerical calculations, but it is, of course, noted that it reduces simply to unity for the Blasius, shear, and magnetic profiles.

RESULTS AND DISCUSSION

THE BLASIUS PROFILE

The reproduction of the stability curves for the Blasius boundary-layer profile is generally considered as a reliable criterion of the basic validity of a stability computational scheme. Accordingly, the stability of the Blasius profile was computed, and the results are compared in figure 7 with those of C. C. Lin as taken from reference (5). For figure 7 the complete stability loop for the Blasius profile was computed with a chosen boundary-layer thickness, δ, of $5\bar{x}/\sqrt{Re_x}$, whereas Lin in reference (5) used a thickness of $6\bar{x}/\sqrt{Re_x}$. It is indicated in reference (5) that greater accuracy is to be expected when the edge of the boundary layer is farther from the solid wall; hence, the value of a direct comparison of the two loops is slightly diminished. The two loops, however, are very similar with the main difference occurring in the tip of the loops and a small difference in the minimum critical Reynolds number. It has been suggested in reference (13) that difficulties may be encountered when α and c are simultaneously large, as is the case at the tip of the loop, but the necessary calculations to explore this possible explanation of differences have not been undertaken. It is noted that the present method uses an α development only around the critical layer singularity, and there it uses α terms up to fourth order.

The value of the minimum critical Reynolds number given in reference (5) is $Re_{\theta,m} = 162$ ($Re_{\delta,m}^* = 421$), whereas the present value with $\delta = 5\bar{x}/\sqrt{Re_x}$ is $Re_{\theta,m} = 147$ ($Re_{\delta,m}^* = 382$) or approximately a ten percent difference. A brief investigation was conducted to determine quantitatively the influence of increasing the chosen value of boundary-layer thickness on the minimum critical Reynolds/number. In addition to the run with $\delta = 5\bar{x}/\sqrt{Re_x}$, runs were made with $\delta = 6\bar{x}/\sqrt{Re_x}$ and $\delta = 10\bar{x}/\sqrt{Re_x}$. In the latter two cases the minimum critical Reynolds numbers were found to be $Re_{\theta,m} = 158$ ($Re_{\delta,m}^* = 411$) and $Re_{\theta,m} = 159$ ($Re_{\delta,m}^* = 415$). It does, therefore, appear that most of the difference between the present and reference (5) values of minimum critical Reynolds number can be attributed to the difference in chosen value of the boundary-layer thickness. Also, for this specific profile, it does not appear that there is a significant change when values of $\dfrac{\delta\sqrt{Re_x}}{\bar{x}}$ greater than six are chosen.

FOREIGN GAS INJECTION EFFECTS

The primary objective of the investigation of the stability of the boundary-layer profiles with foreign gas injection was to

determine the effect of the different foreign gases on the minimum critical Reynolds number at various wall-to-free-stream temperature ratios. To accomplish this objective it was necessary to determine the eigenvalues only at the low Reynolds number end of the stability loops and, hence, complete loops are in general not presented. The partial loops for the cases of air injected into air at three wall-temperature ratios are presented in figure 8 which clearly shows the influence of boundary-layer cooling on the stability of small disturbances. Here we observe that in going from a hot wall (T_w = 2.0) to a cold wall (T_w = 0.5) there is almost a three order of magnitude increase in the minimum critical Reynolds number and that the maximum value of α for neutral stability is decreased by a factor of two. These results are very similar to the results presented by Lees in reference (17). However, these are for Mach number zero and include air injection. His results were for a Mach number of 0.7 without air injection. As may be seen in figures 9 and 10 the form and variation with wall temperature of the stability loops (i.e. the tendency for the loops to encompass a larger range of wave numbers and for the minimum critical Reynolds numbers to decrease with increased T_w) for CCl_4 injection and for no injection are very similar to that shown in figure 8. With helium injection the increase of the minimum critical Reynolds number with decrease of wall-temperature ratio is considerably less pronounced, and the form of the stability loops differs from the previous loops as in figure 11. For loops of this form it is, in fact, possible that the lower wall-temperature ratio boundary-layer profiles may experience an earlier transition to turbulence than the profiles with higher temperature ratios even though they exhibit a larger minimum critical Reynolds number. This could occur because the higher wave numbers would produce a greater amplification rate of the small disturbances. It should be noted, however, that these results occur at very low values of $\alpha_\delta R_\delta$, and since the validity of the viscous solutions is based on neglecting higher order terms in an expansion in $1/\sqrt{\alpha_\delta R_\delta}$, there must be some reservation about their accuracy. In fact, the helium results for a wall temperature ratio of 2.0 yield a product $\alpha_\delta R_\delta$ at the minimum critical Reynolds number which is roughly a factor of three lower than any other values calculated herein. In an effort to investigate more fully the trend, an additional run with a wall-temperature ratio of 1.5 was inserted. The lowering of the stability loops with increased wall-temperature ratio, as indicated by the T_w = 1.5 and 2.0 curves, appears to be a substantiated trend; but its physical causes are not fully understood.

The stability loops at a wall-temperature ratio of 0.5 for the three injected gases are compared with the zero injection stability loop in figure 12. It is seen that for all injected gases the instability area within the loop appears to be increased in comparison to the zero injection case. More significant,

however, is the fact that the large molecular weight and diameter gas, CCl_4, has the highest minimum critical Reynolds number. This result quantitatively confirms the prediction of the "inviscid criterion" by Shen, reference (1). If we couple this result with the results indicated by Korobkin, reference (2), it appears that mass transfer systems using a gas with a favorable combination of large molecular weight and diameter may have considerable promise.

It is further observed in figure 12 that at the wall temperature ratio of 0.5 the minimum critical Reynolds number for the boundary layer with helium injection is more than an order of magnitude lower than that of the CCl_4 injection boundary layer. In figure 13 we present a summary plot which compares the minimum critical Reynolds number at three wall-temperature ratios. The favorable advantage of the CCl_4 over the He as an injected gas is maintained at all temperature ratios, but it is considerably decreased in magnitude as the temperature ratio is increased. In fact, at a wall temperature ratio of 2.0 the minimum critical Reynolds number for the He injection profile is greater than that of both the air profiles (i.e. with and without air injection) and is almost equal to that of the CCl_4 profile. As has been previously indicated, all of the preceding comparisons have been made for a single value of the injection rate parameter, i.e. $f(0) = 0.1$. No consideration has been given to the fact that in practical applications different values of $f(0)$ would be used for the different foreign gases. Stability comparison for design applications should, therefore, be made on the basis of the injection rate parameter which is needed to meet a specific cooling requirement.

SHEAR AND MAGNETOHYDRODYNAMIC EFFECTS

The comparative stability loops for the shear and magnetohydrodynamic profile are given in figure 14. Since the use of the momentum thickness as defined by equation (49) is somewhat vague, the value of the minimum critical Reynolds number based on distance from the leading edge of the plate, $\bar{x}$, is also indicated on figure 14. The use of $\bar{x}$ instead of $\bar{\theta}$ as a reference length does not alter the relative stability of the profiles. It is observed that the use of a magnetic field with the parameter $b = 0.1$ increases the minimum critical Reynolds number of the Blasius boundary-layer profile by one or two orders of magnitude depending on the choice of $\bar{\theta}$ or $\bar{x}$ as a reference length. This result is essentially the same as Rossow's, reference (4), and agrees quantitatively within the accuracy of one's ability to read and extrapolate the reference (4) curves.

The effect of the external vorticity for the shear parameter ξ^* equal to 0.1 on the stability of the Blasius or on the magnetohydrodynamic boundary layer is comparatively small. On the basis

20

of length minimum critical Reynolds numbers, $Re_{x,m}$, the shear increases the stability of the Blasius profile by about thirty percent. The shear, which as an incremental effect, changes both the Blasius and the magnetohydrodynamic profiles in a similar manner and might have been expected to have the same effect on the stability of both profiles; however, the detailed calculations did not substantiate this expectation. In fact, $Re_{x,m}$, for the magnetohydrodynamic profile was decreased by about forty percent. While this as yet unexplained result is of interest, it is considered more important to emphasize that for a value of the shear parameter, $\xi^* = 0.1$, one may expect percentage rather than order of magnitude changes in the minimum critical Reynolds number of the boundary layer.

CONCLUSIONS

The present results show that the injection at a blowing rate, $f(0) = 0.1$, of a large molecular weight gas such as CCl_4 may actually result in a stabilization of the laminar boundary layer. The stabilization in terms of increase in minimum critical Reynolds number when compared with the zero blowing values indicated a 35 percent increase for a wall temperature ratio of 2.0 and became a 28 percent increase at a wall temperature ratio of 0.5. This result tends to substantiate the indications of the "inviscid criterion" set forth by Shen in reference (1).

The injection of helium, a small-diameter light-weight gas, was generally destabilizing when compared with zero blowing values except for the high wall-temperature ratios. Such a comparison shows that the stability in terms of minimum critical Reynolds number with helium injection was reduced to about five percent of the zero blowing value at a wall-temperature ratio of 0.5; however, at a temperature ratio of 2.0 the helium injection actually increased the stability by 15 percent. While the results with helium injection again generally tend to substantiate the "inviscid criterion," it is observed that they fail to do so at high wall-temperature ratios. This result might well be expected since indications obtained for an infinite Reynolds number need not necessarily define conditions at a finite Reynolds number (i.e. at the low Reynolds number end of the stability loops) for all cases considered. Accordingly, it appears that while the "inviscid criterion" are generally reliable, their indiscriminate use could produce misleading results. This conclusion, which is believed to be reasonable, must be tempered by the fact that it is based on results obtained at very low values of αR.

The investigation of the influence of small external shear on the stability of laminar boundary layers indicated that only

percentage, rather than order of magnitude changes in the mini-
mum critical Reynolds number, would be expected for the cases
herein considered. Quantitatively, the external vorticity
characterized by a shear parameter, ξ^*, of one-tenth increased
the minimum critical Reynolds number based on length of the
Blasius profile by 30 percent, whereas the same shear reduced
the stability of the magnetohydrodynamic profile by 40 percent.
In contrast to these percentage changes it is noted that the
application of a magnetic field characterized by a magnetic
parameter, b, of one-tenth, increased the Blasius profile length
minimum critical Reynolds number by two orders of magnitude from
$Re_{x,m} = 5.2 \times 10^4$ to $Re_{x,m} = 3.1 \times 10^6$.

Quantitative values have been determined which show the
influence on the calculated minimum critical Reynolds number of
different choices of the Blasius variable which is used to
define the outer edge of the boundary layer. Specifically,
for η equal to five, six, or ten, the values of $Re_{\theta,m}$ were
respectively, 147, 158, or 159. It is apparent that there is
only a negligible improvement if values of η greater than six
are used.

REFERENCES

(1) Shen, S. F., "The Theory of Stability of Compressible
     Laminar Boundary Layers with Injection of a Foreign Gas,"
     NAVORD Report 4467, May 1957

(2) Korobkin, I., "The Effects of the Molecular Properties of
     an Injected Gas on Compressible Air Laminar Boundary Layer
     Skin Friction and Heat Transfer," NAVWEPS Report 7410,
     March 1961

(3) Harris, E. L., "Effect of Free-Stream Shear on an
     Incompressible, Flat-Plate, Magnetohydrodynamic Laminar
     Boundary Layer," NOLTR 61-60, April 1962

(4) Rossow, V. J., "Boundary-Layer Stability Diagrams for
     Electrically Conducting Fluids in the Presence of a
     Magnetic Field," NASA TR R-37, 1959

(5) Lin, C. C., "On the Stability of Two-Dimensional Parallel
     Flows," Quart. of Appl. Math.; Part I - "General Theory,"
     Vol. III, No. 2, July 1945; Part II - "Stability in an
     Inviscid Fluid," Vol. III, No. 3, October 1945; Part III -
     "Stability in a Viscous Fluid," Vol. III, No. 4, January 1946

(6) Dunn, D. W., and Lin, C. C., "On the Stability of the
     Laminar Boundary Layer in a Compressible Fluid," JAS, Vol. 22,
     No. 7, July 1955

(7) Reshotko, E., "Stability of the Compressible Laminar
     Boundary Layer," Guggenheim Aeronautical Laboratory, CIT,
     Hypersonic Research Project Memo No. 52, 15 January 1960

(8) Lock, R. C., "The Stability of the Flow of an Electrically
     Conducting Fluid Between Parallel Planes Under a Transverse
     Magnetic Field," Proc. Roy. Soc. London, Ser. A, Vol. 233,
     No. 1192, pp. 105-125, December 1955

(9) Timman, R., Zaat, J. A., and Burgerhout, T. J., "Stability
     Diagrams for Laminar Boundary Layer Flow," NLL-TN F. 193,
     National Luchtvaartlaboratorium, October 1956

(10) Lin, C. C., "The Theory of Hydrodynamic Stability,"
     Cambridge University Press, 1955

(11) Lees, L. and Lin, C. C., "Investigation of the Stability
     of the Laminar Boundary Layer in a Compressible Fluid,"
     NACA TN 1115. September 1946

(12) Brown, W. B., "Exact Numerical Solution of the Complete
     Linearized Equations for the Stability of Compressible
     Boundary Layers," presented to 1961 meeting of APS, Fluid
     Mechanics Division, Berkeley, California, 20 November 1961,
     NOR 62-15 (BLC-137)

(13) Mack, L. M., "Numerical Calculation of the Stability of
     the Compressible Laminar Boundary Layer," JPL, CIT, Report
     No. 20-122, May 1960

(14) Holstein, H., "Uber die Aussere and Innere Reibungsschict
     bei Storungen Laminarer Stromungen," ZAMM 30, 25-49, 1950

(15) Butler, J. F., "A Fortran II (IBM 704) Subroutine for the Solution of Ordinary Differential Equations with Automatic Linkage, Termination and Output Features," NAVORD Report 6701, Math Department Report M-6, 7 October 1959

(16) Hirschfelder, J. O., Curtiss, C. F., and Bird, R. B., "Molecular Theory of Gases and Liquids," John Wiley and Sons, 1954

(17) Lees, L., "The Stability of the Laminar Boundary Layer in a Compressible Fluid," NACA TN 1360, July 1947
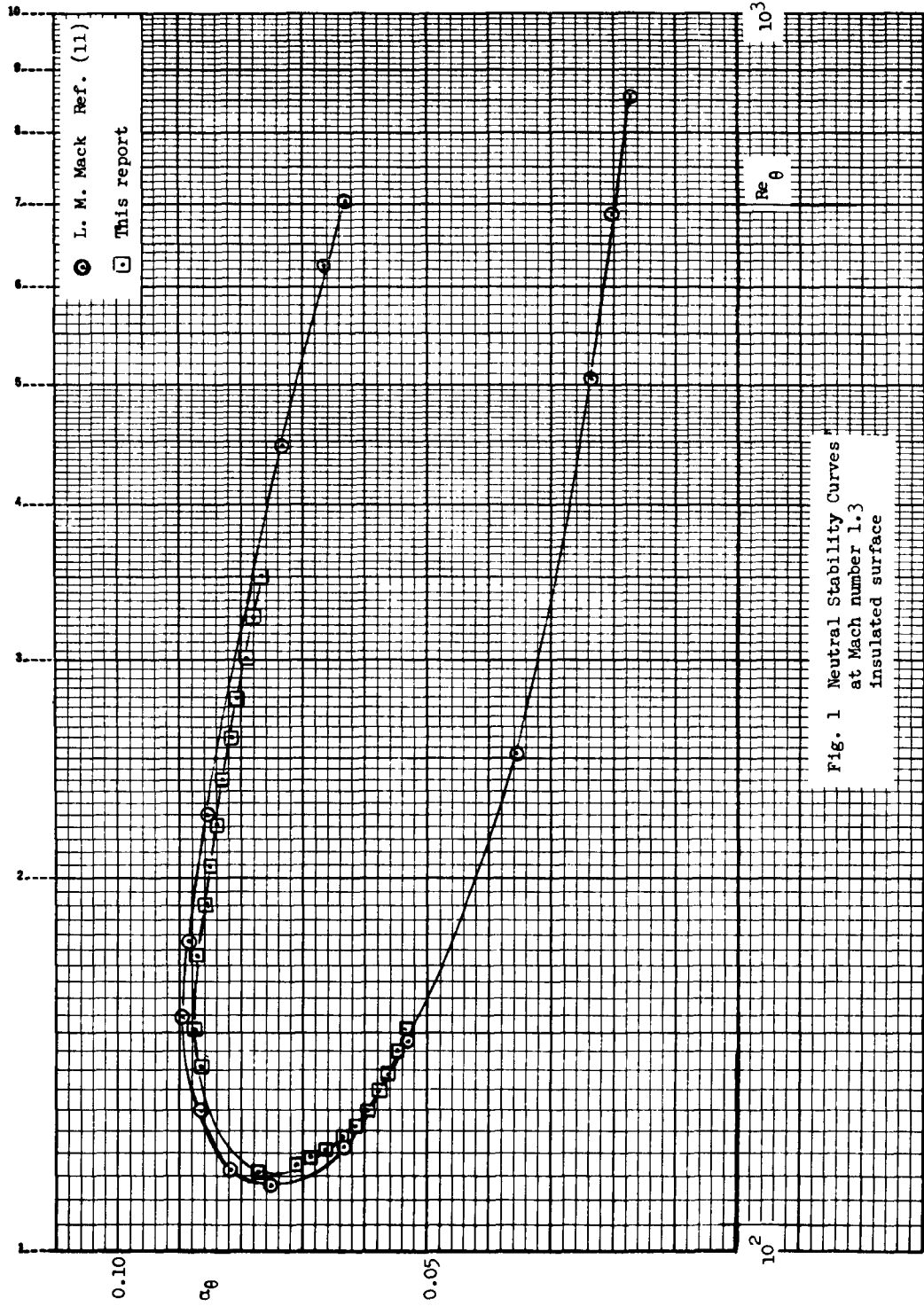
Fig. 1 Neutral Stability Curves
at Mach number 1.3
insulated surface

Fig. 2 Non-Dimensional Boundary-Layer Profiles
with No Injection for Different Wall to
Free-Stream Temperature Ratios, T_w

Fig. 2a Velocity Profiles

Fig. 2b   Temperature Profiles
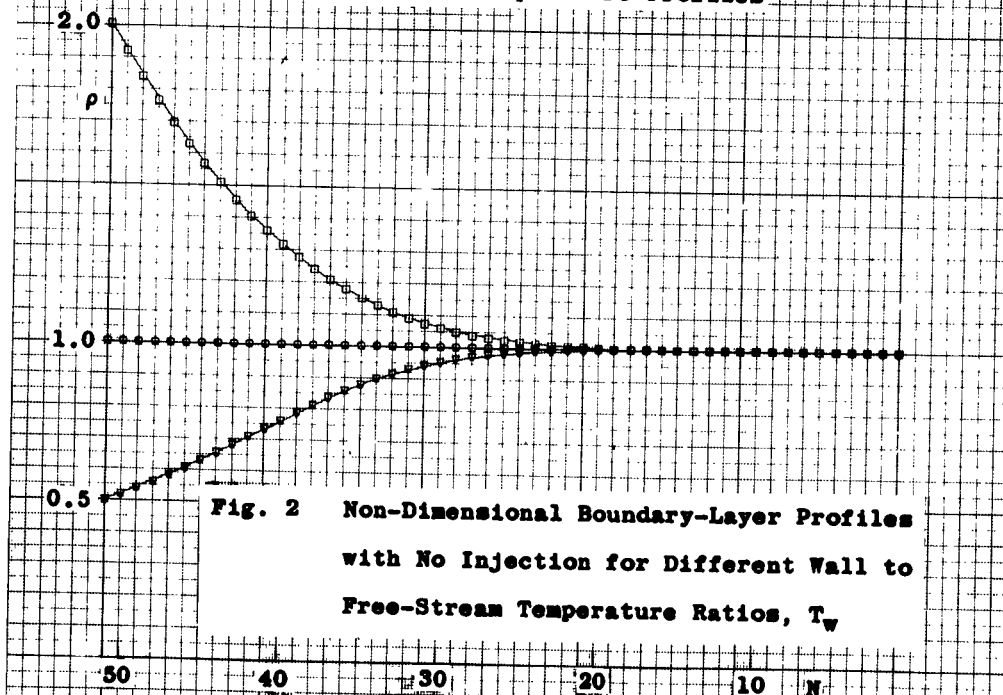
Fig. 2   Non-Dimensional Boundary-Layer Profiles
with No Injection for Different Wall to
Free-Stream Temperature Ratios, T_W

Fig. 2c   Density Profiles
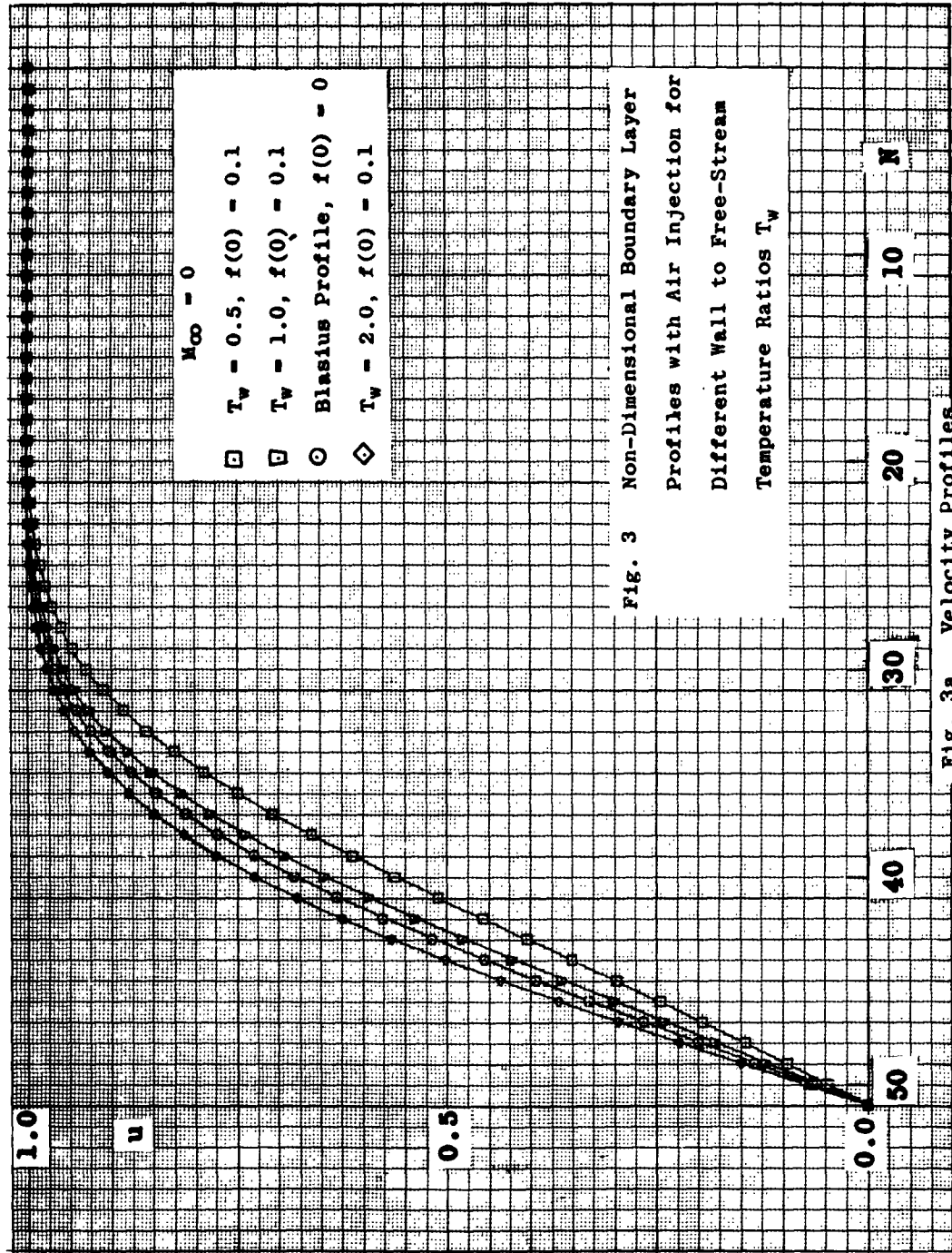
Fig. 3 Non-Dimensional Boundary Layer
Profiles with Air Injection for
Different Wall to Free-Stream
Temperature Ratios T_w

Fig. 3a Velocity Profiles
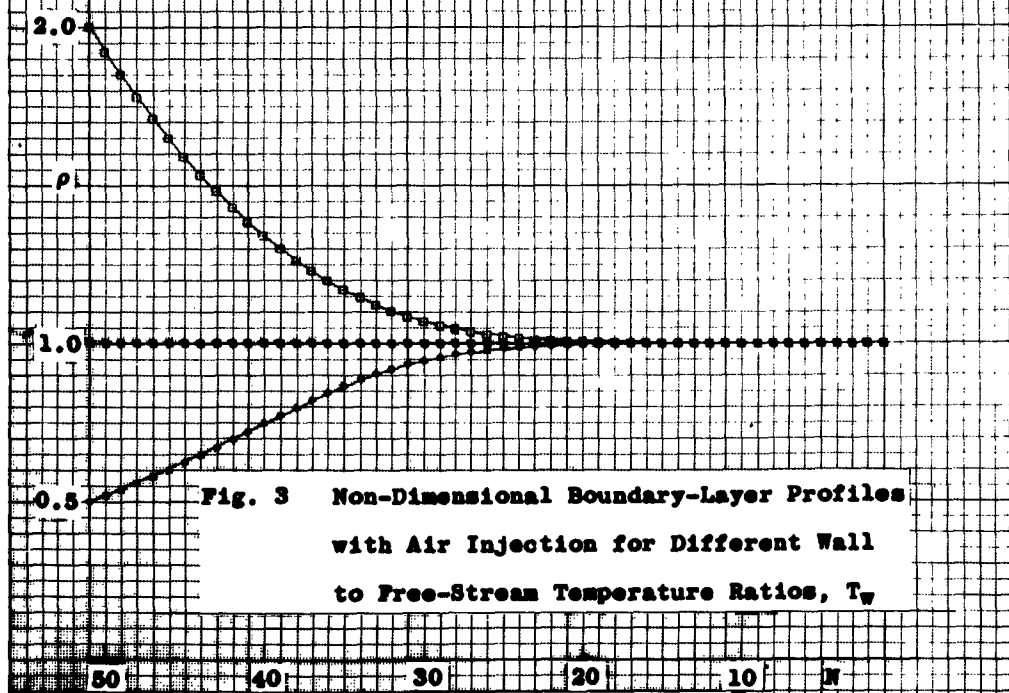
$M_\infty = 0$

☐ $T_w = 0.5$, $f(0) = 0.1$

☐ $T_w = 1.0$, $f(0) = 0.1$

⊙ Blasius Profile, $f(0) = 0$

◇ $T_w = 2.0$, $f(0) = 0.1$

Fig. 3b   Temperature Profiles

Fig. 3   Non-Dimensional Boundary-Layer Profiles with Air Injection for Different Wall to Free-Stream Temperature Ratios, T_w

Fig. 3c   Density Profiles
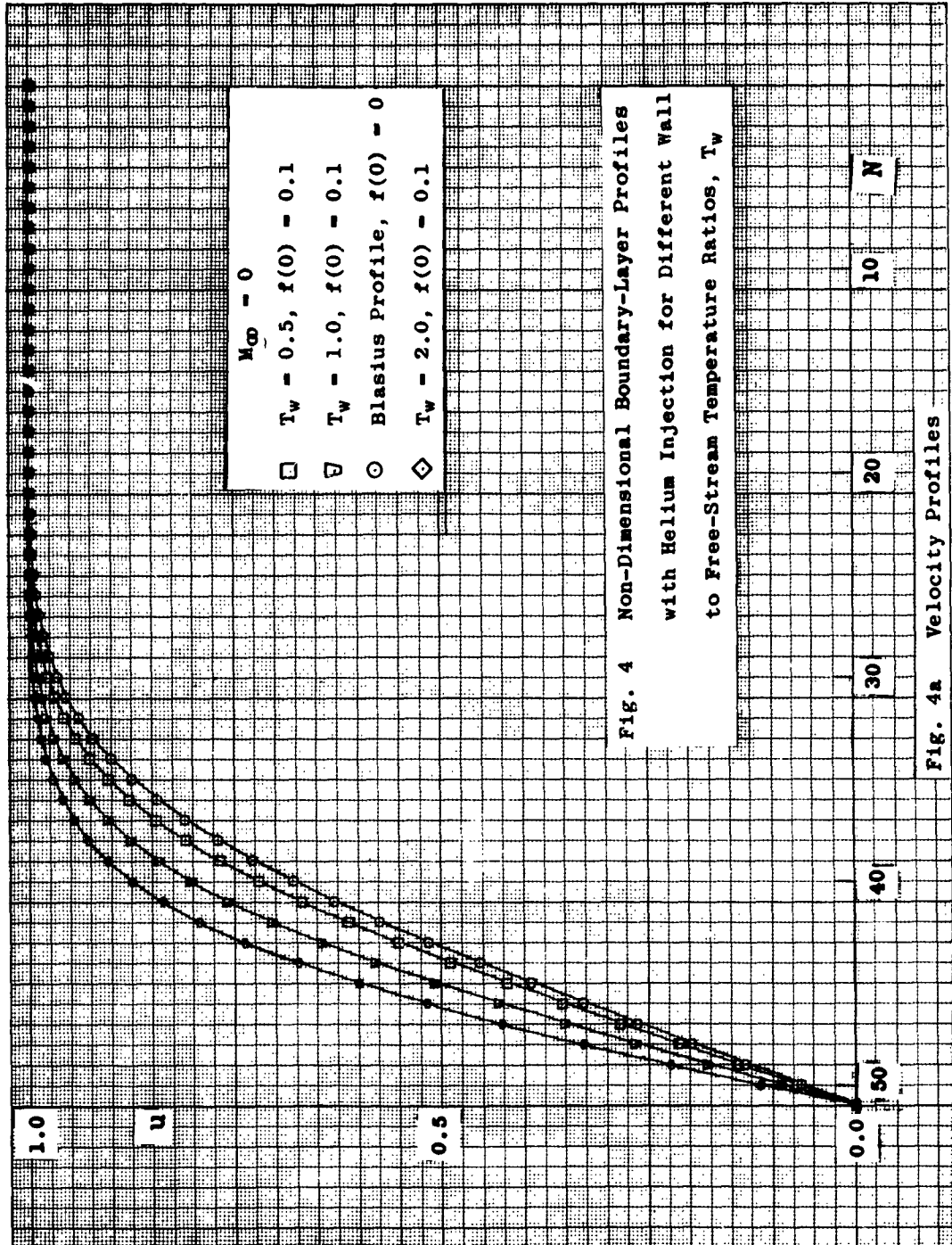
Fig. 4   Non-Dimensional Boundary-Layer Profiles with Helium Injection for Different Wall to Free-Stream Temperature Ratios, T_w

$M_\infty = 0$

□ $T_w = 0.5$, $f(0) = 0.1$
◁ $T_w = 1.0$, $f(0) = 0.1$
⊙   Blasius Profile, $f(0) = 0$
◇ $T_w = 2.0$, $f(0) = 0.1$

Fig. 4a   Velocity Profiles

Fig. 4b   Temperature Profiles

Fig. 4   Non-Dimensional Boundary-Layer Profiles
with Helium Injection for Different Wall
to Free-Stream Temperature Ratios, T_w

Fig. 4c   Enthalpy Profiles

Fig. 4d   Density Profiles

$M_\infty = 0$

☐ $T_w = 0.5$, $f(0) = 0.1$

☑ $T_w = 1.0$, $f(0) = 0.1$

⊙   Blasius Profile, $f(0) = 0$

◇ $T_w = 2.0$, $f(0) = 0.1$
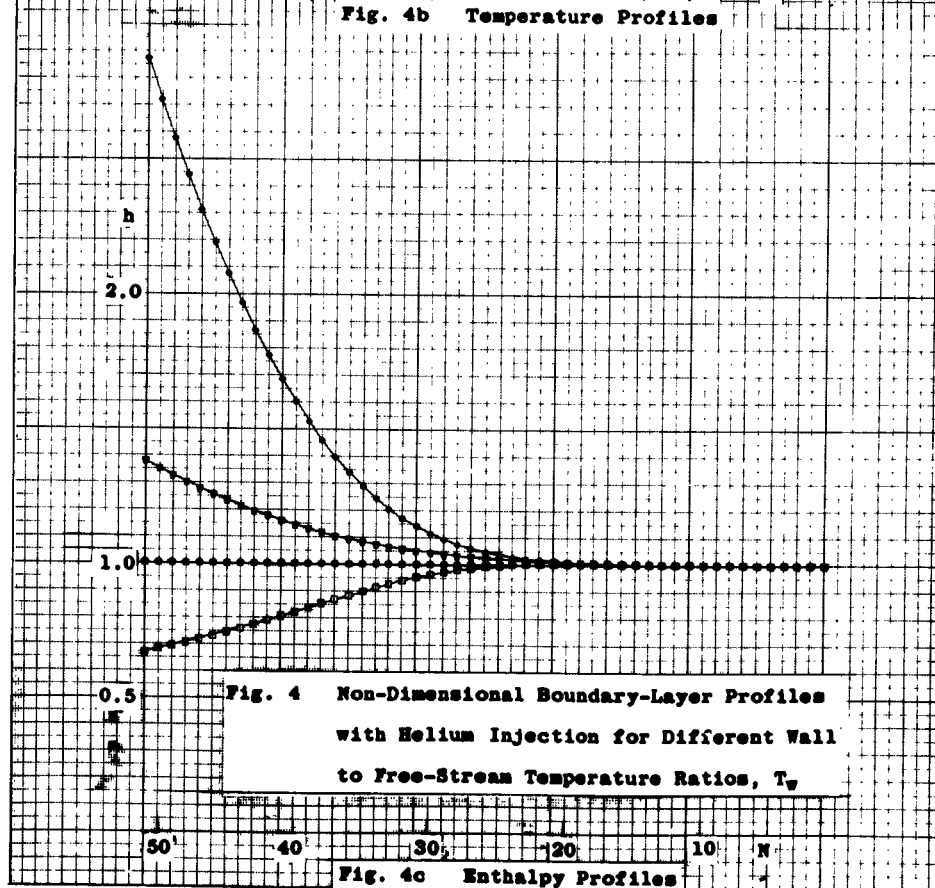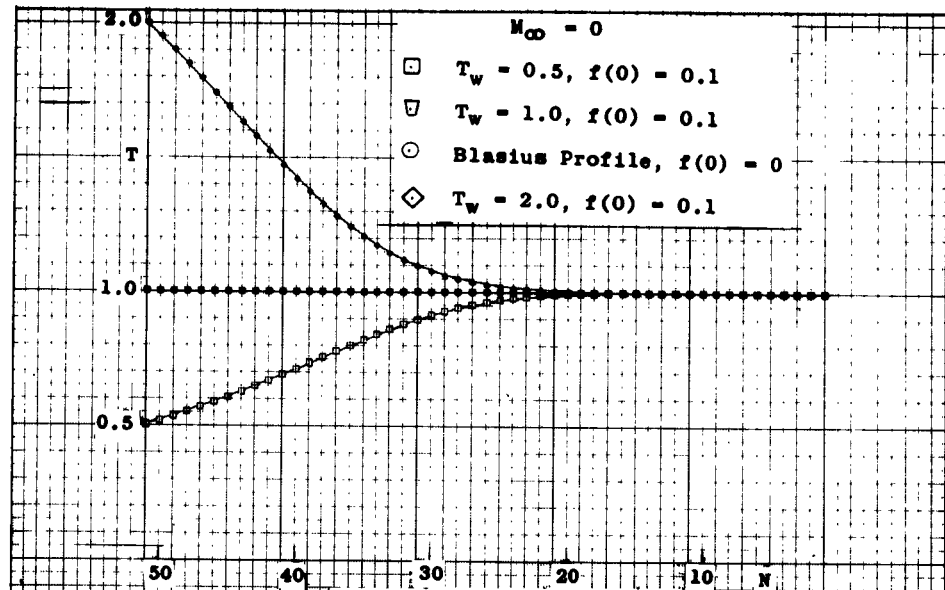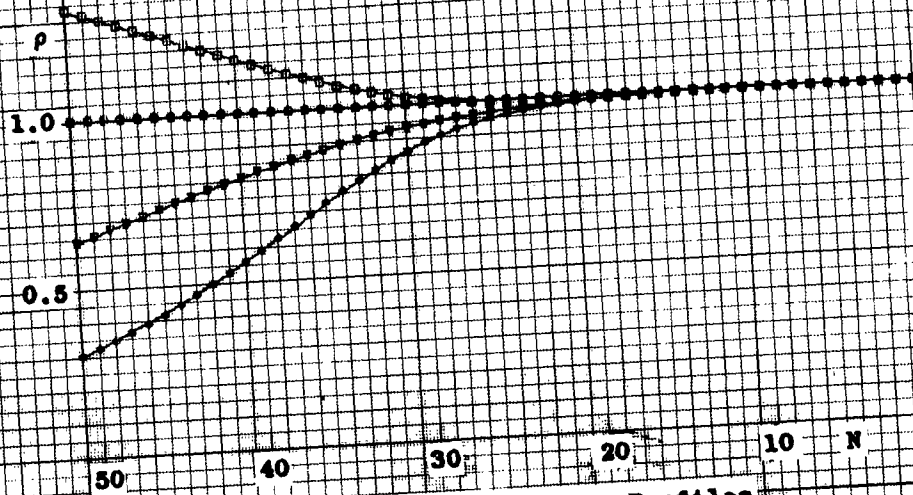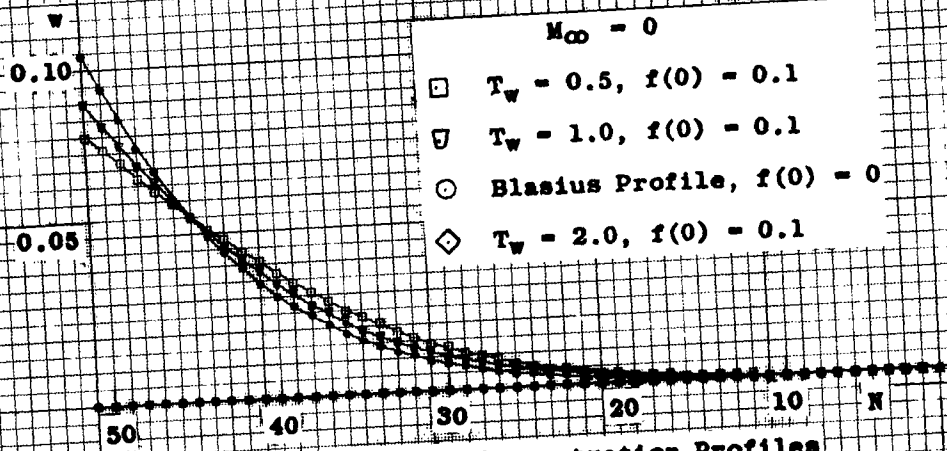
Fig. 4e   Concentration Profiles

Fig. 4   Non-Dimensional Boundary-Layer Profiles
with Helium Injection for Different Wall
to Free-Stream Temperature Ratios, T_w

Fig. 5 Non-Dimensional Boundary-Layer Profiles with CCl_4 Injection for Different Wall to Free-Stream Temperature Ratios, T_w

Fig. 5a Velocity Profiles

$M_\infty = 0$

☐ $T_w = 0.5$, $f(0) = 0.1$

▽ $T_w = 1.0$, $f(0) = 0.1$

⊙   Blasius Profile, $f(0) = 0$

◇ $T_w = 2.0$, $f(0) = 0.1$
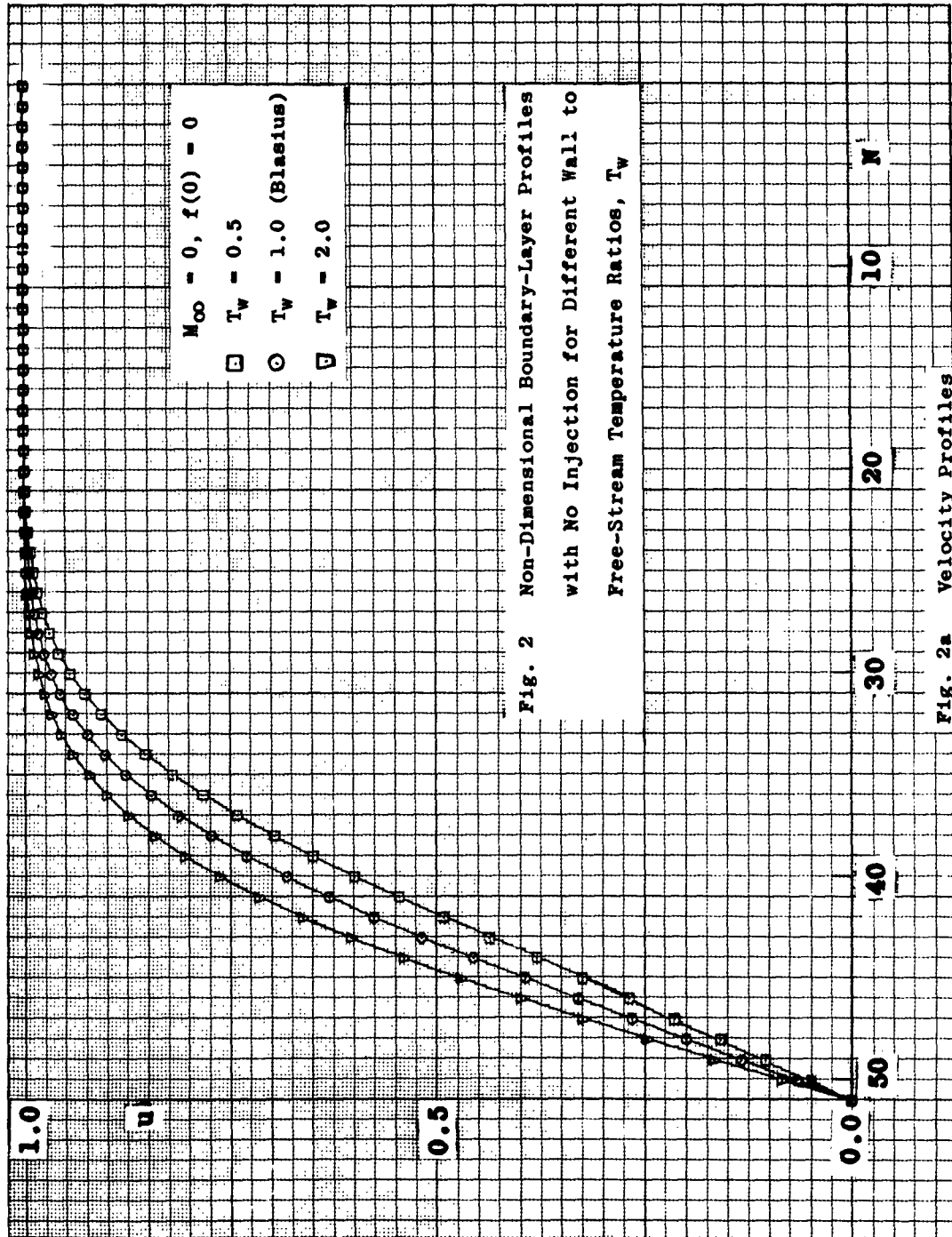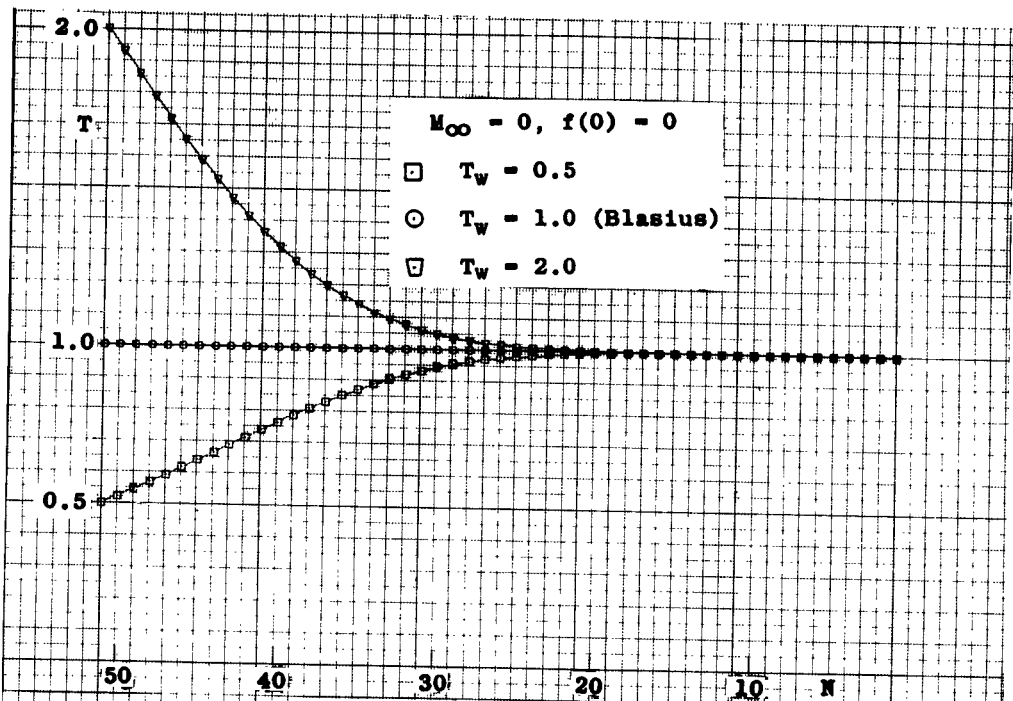
Fig. 5b   Temperature Profiles

Fig. 5   Non-Dimensional Boundary-Layer Profiles with CCl$_4$ Injection for Different Wall to Free-Stream Temperature Ratios, T$_w$

Fig. 5c   Enthalpy Profiles

Fig. 5d   Density Profiles

Fig. 5   Non-Dimensional Boundary-Layer Profiles with CCl$_4$ Injection for Different Wall to Free-Stream Temperature Ratios, T$_w$

Fig. 5e   Concentration Profiles
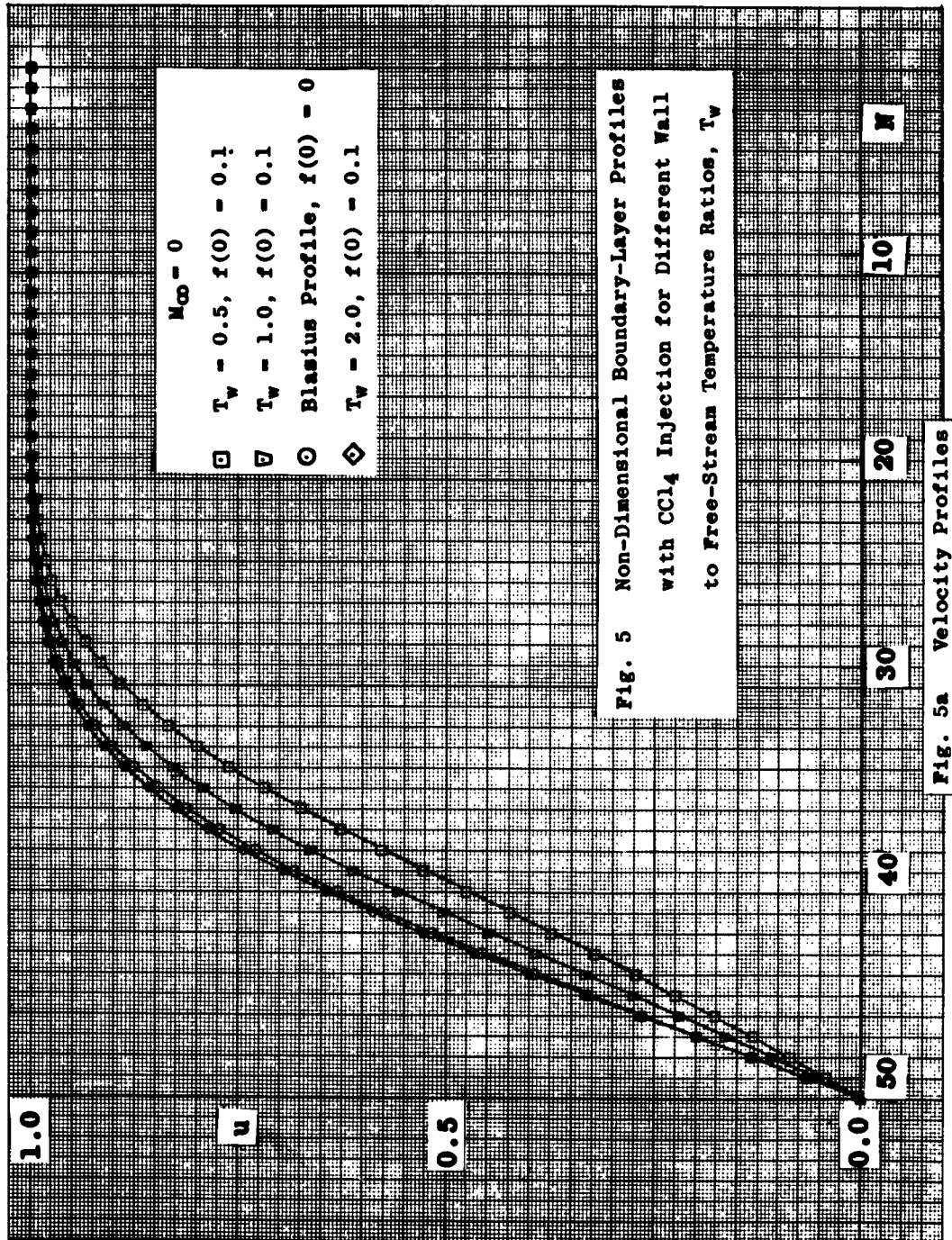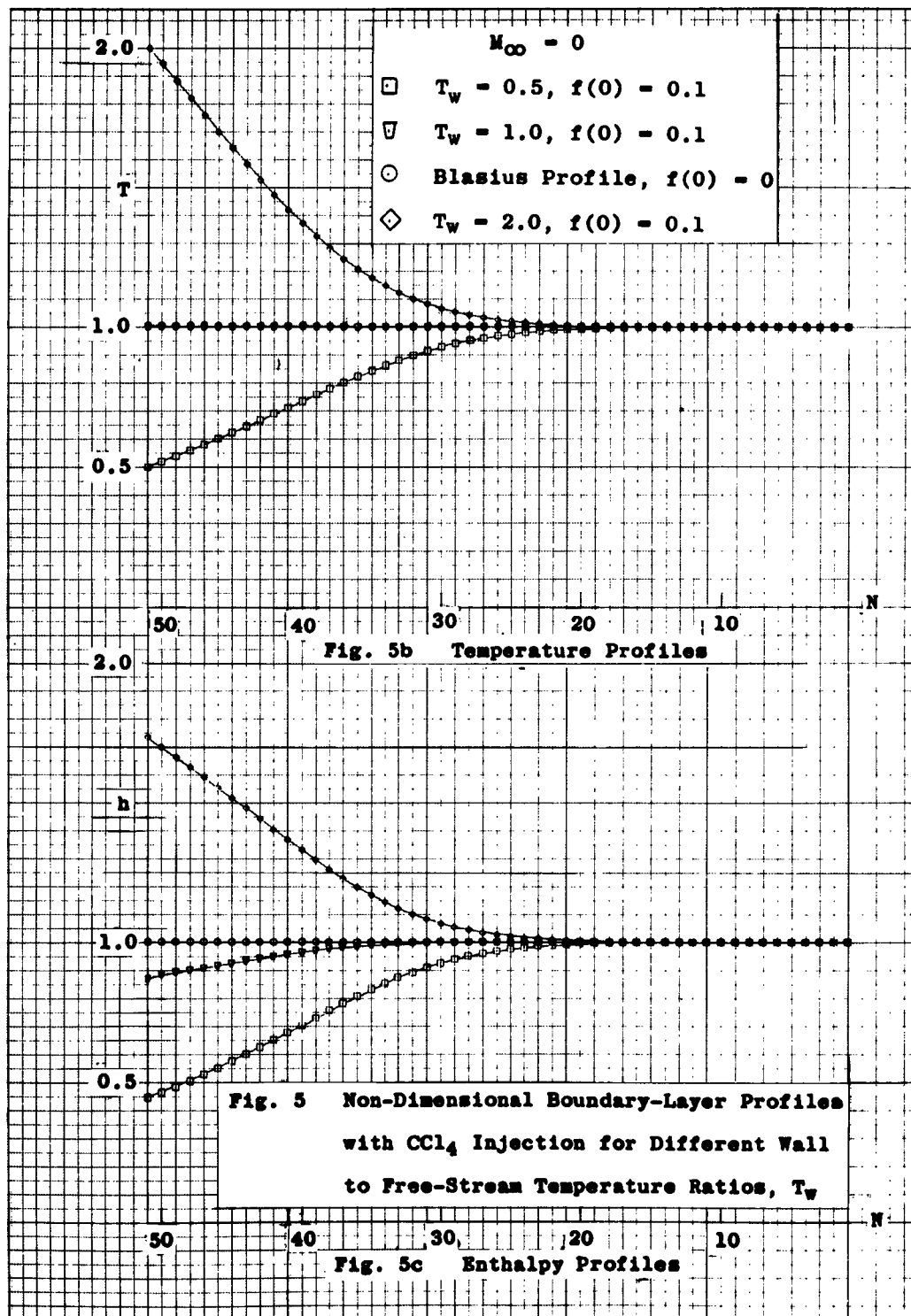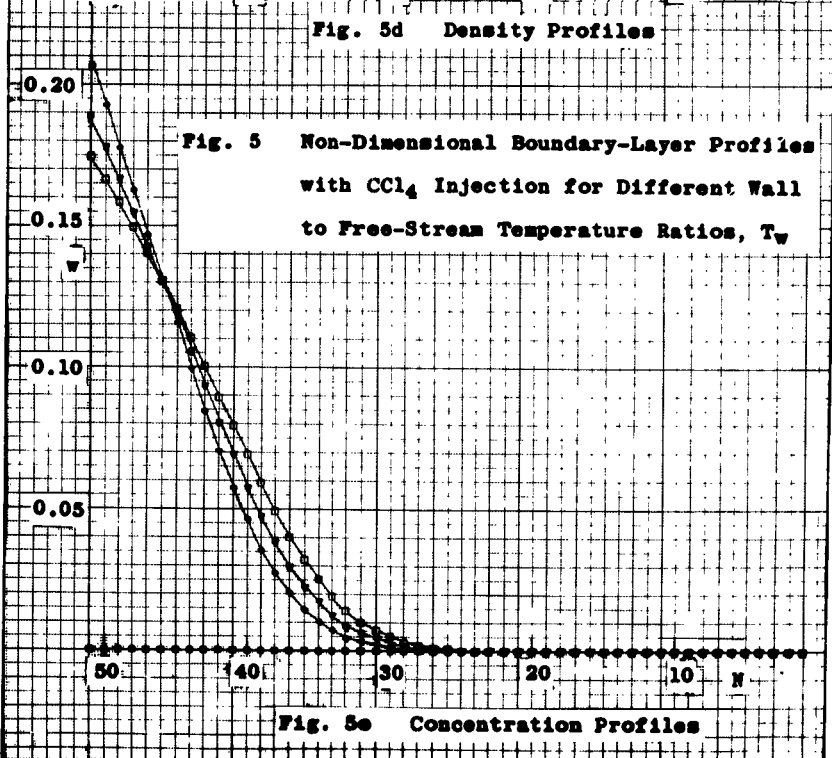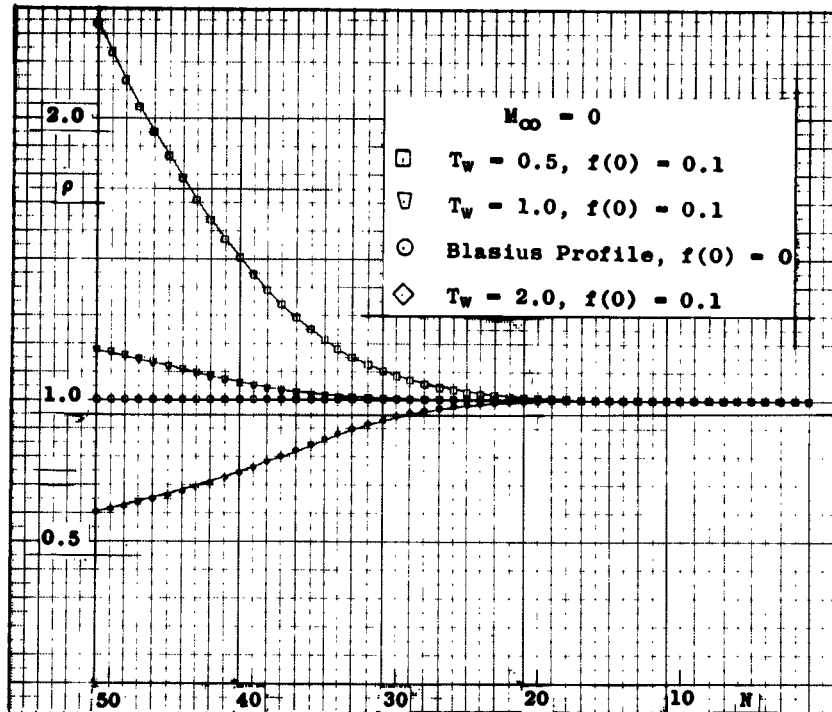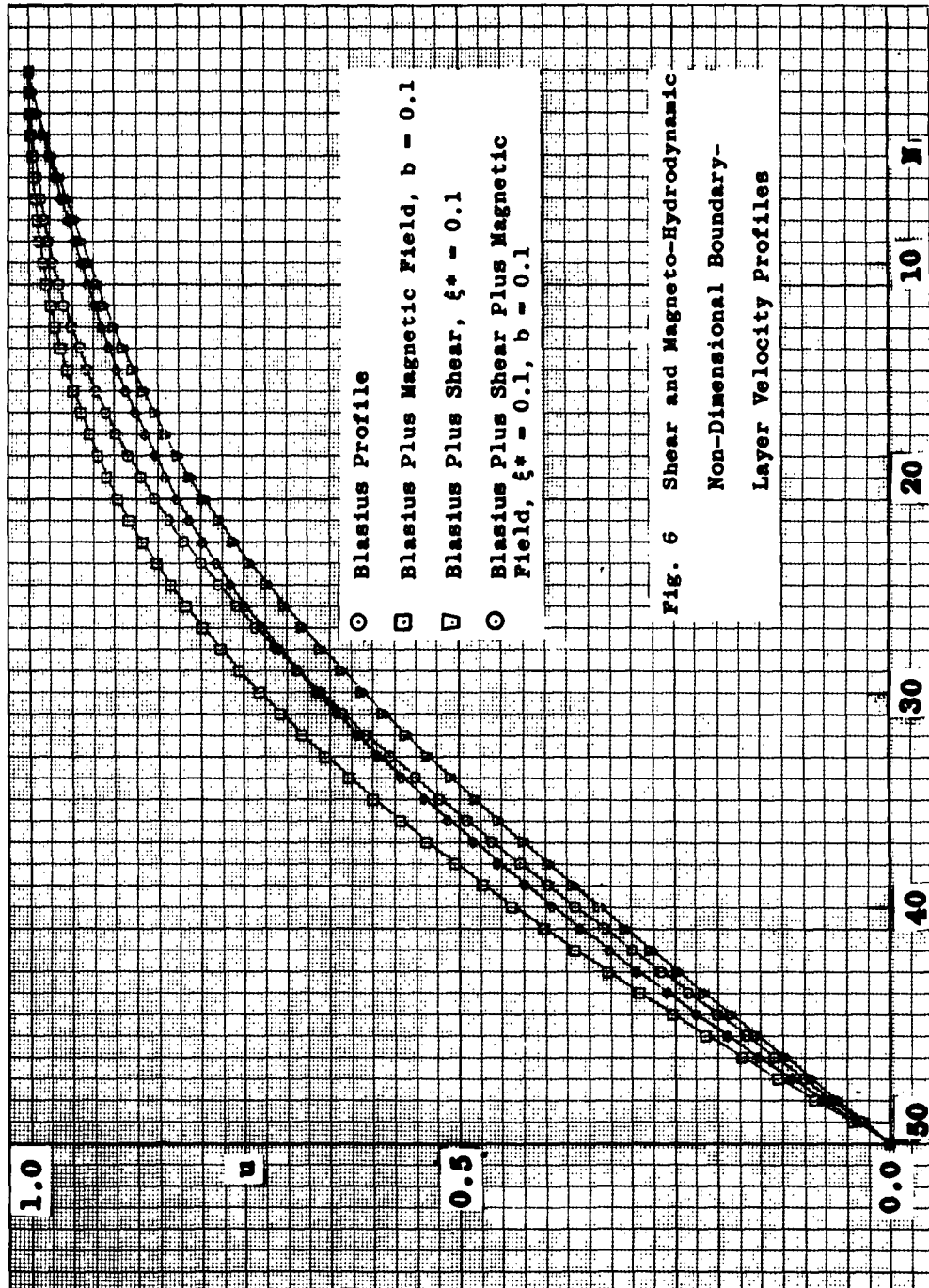
Fig. 6   Shear and Magneto-Hydrodynamic
Non-Dimensional Boundary-
Layer Velocity Profiles

⊙   Blasius Profile

◻   Blasius Plus Magnetic Field, b = 0.1

◺   Blasius Plus Shear, ξ* = 0.1

◉   Blasius Plus Shear Plus Magnetic
Field, ξ* = 0.1, b = 0.1

Fig. 7 Neutral Stability Curves for the Blasius Boundary-Layer Profiles with Effect of Boundary-Layer Thickness,

Fig. 8   Neutral Stability Curves for
Air Injection with Effect of Wall
to Free-Stream Temperature Ratio, T_w

Fig. 9   Neutral Stability Curves for CCl_4 Injection with Effect of Wall to Free-Stream Temperature Ratio, T_w

Fig. 10 Neutral Stability Curves for Zero
Injection with Effect of Wall to
Free-Stream Temperature Ratio, T_w
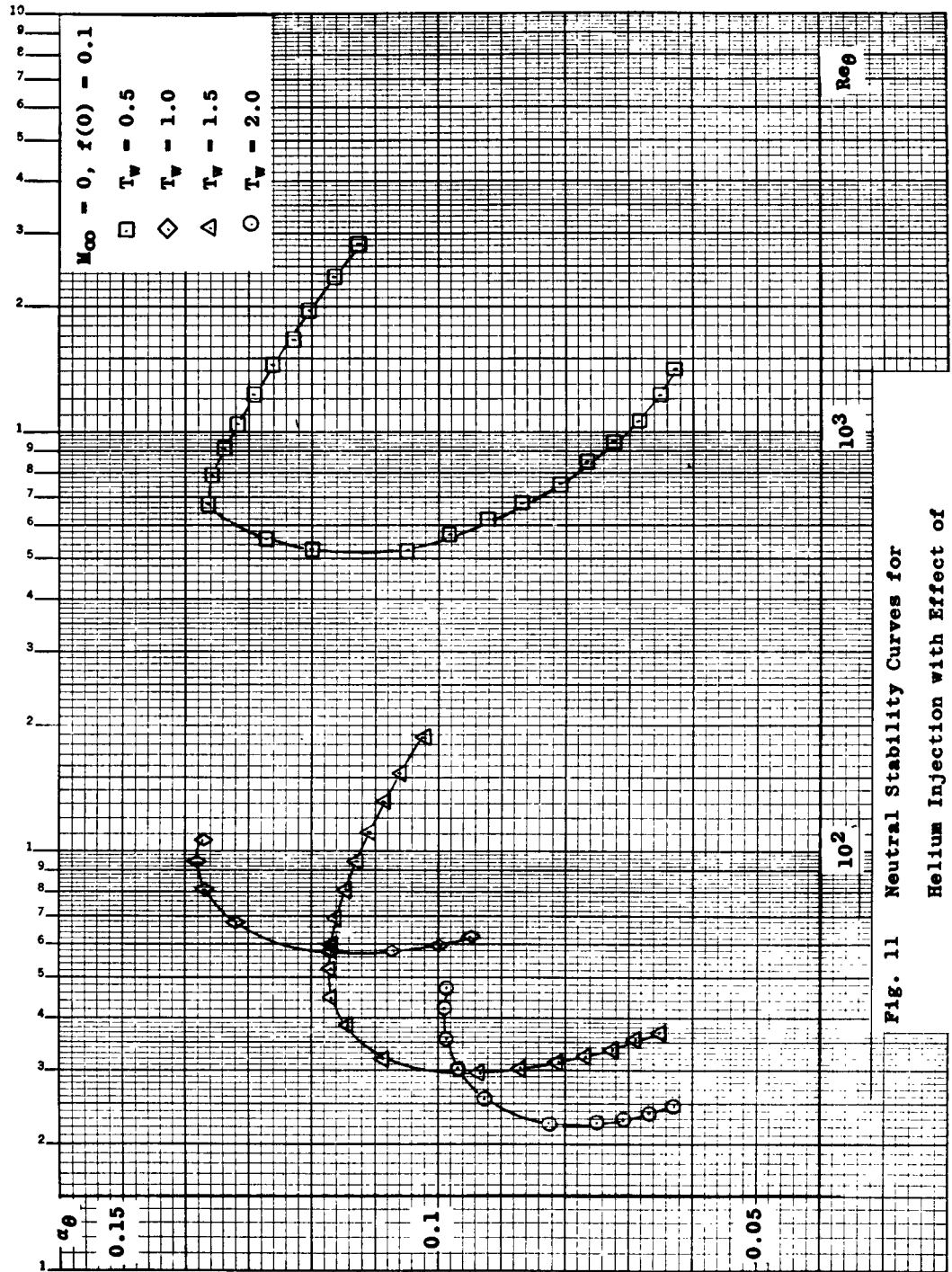
Fig. 11   Neutral Stability Curves for
Helium Injection with Effect of
Wall to Free-Stream Temperature Ratio, T_w

Fig. 12   Neutral Stability Curves for $T_w = 0.5$ with Injection Effects for Different Kinds of Gases
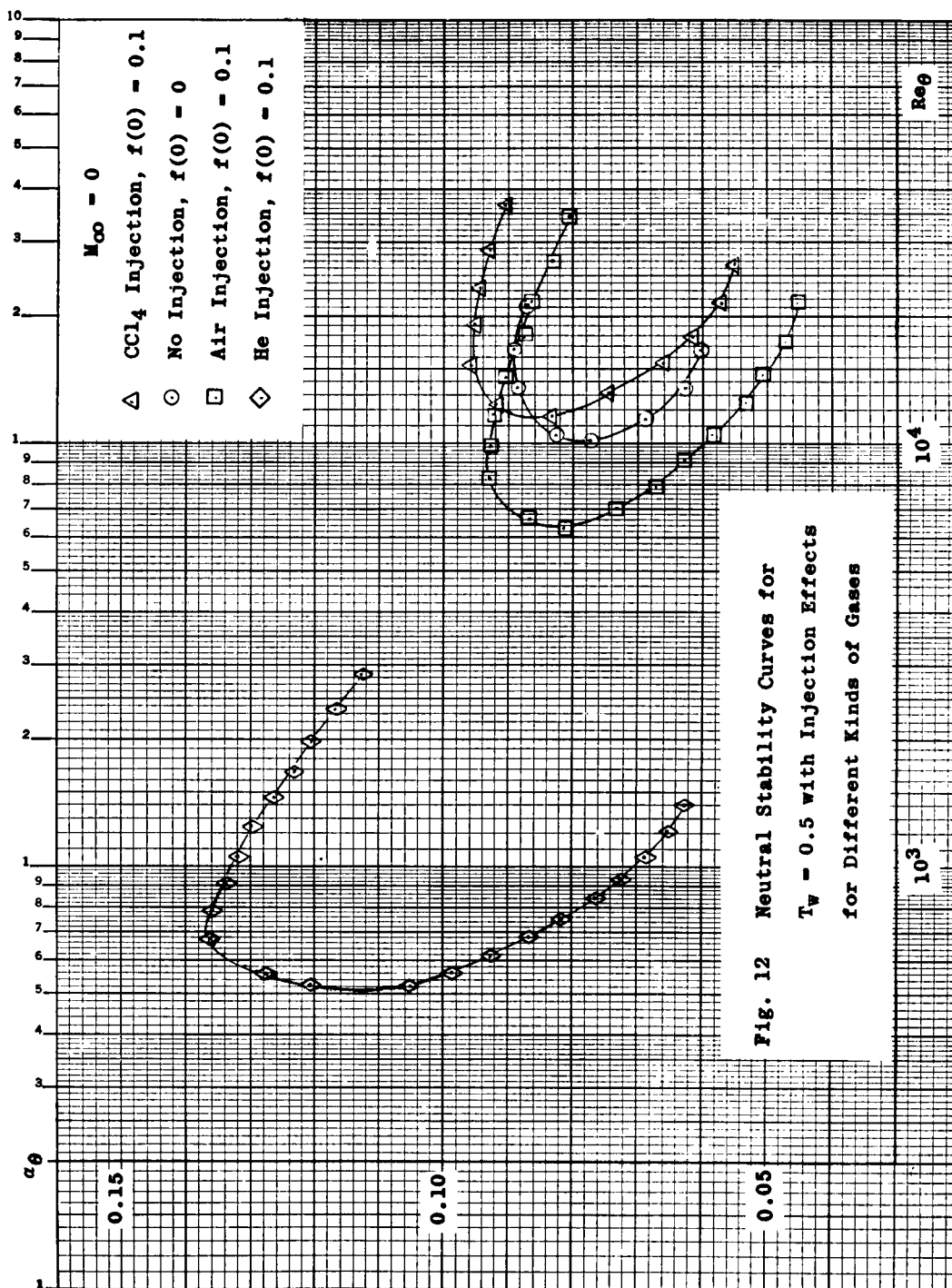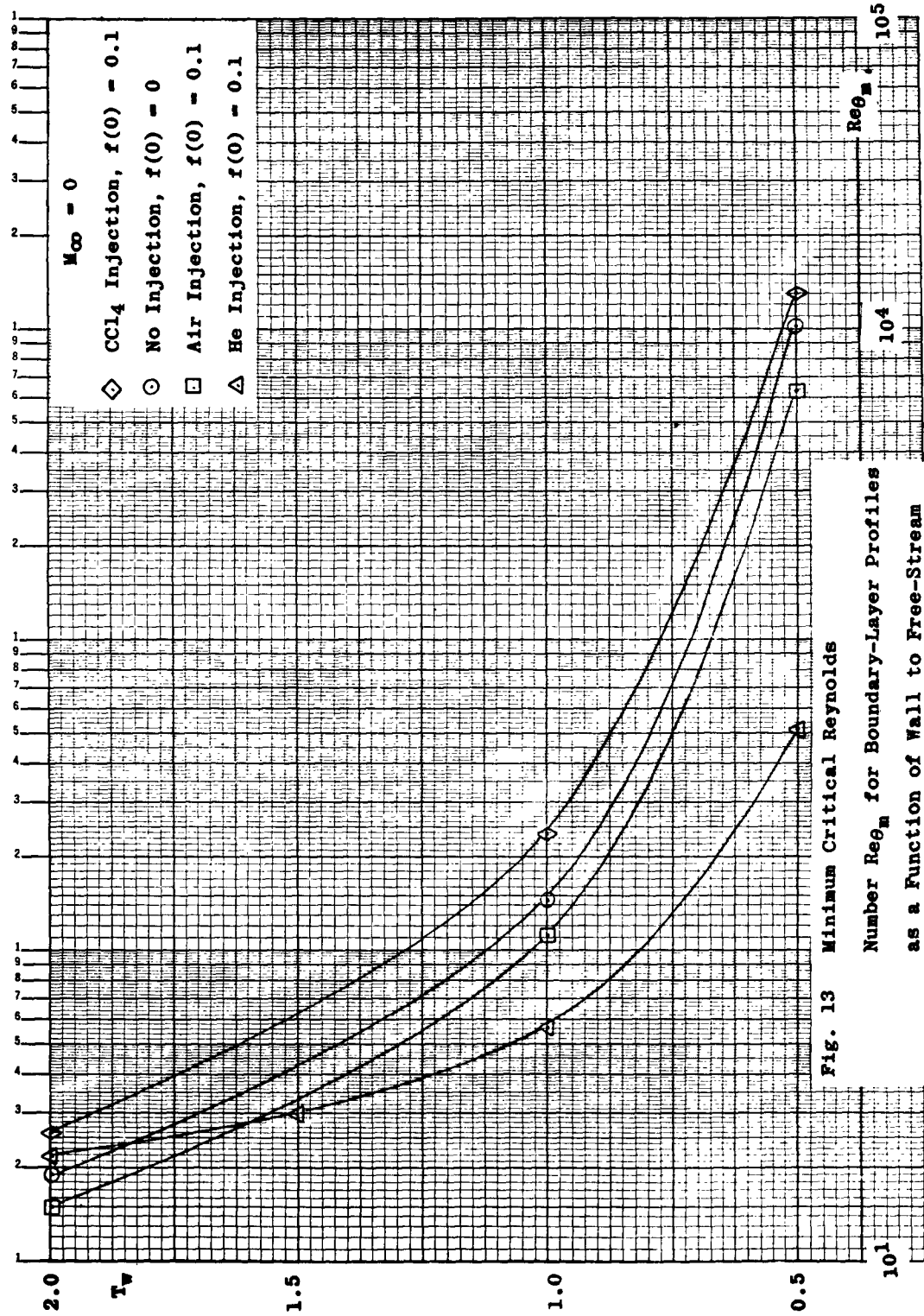
Fig. 13   Minimum Critical Reynolds
Number Re_{θ_m} for Boundary-Layer Profiles
as a Function of Wall to Free-Stream
Temperature Ratio, T_w

Fig. 14   Neutral Stability Curves
for the Shear and Magneto-Hydrodynamic
Boundary-Layer Profiles
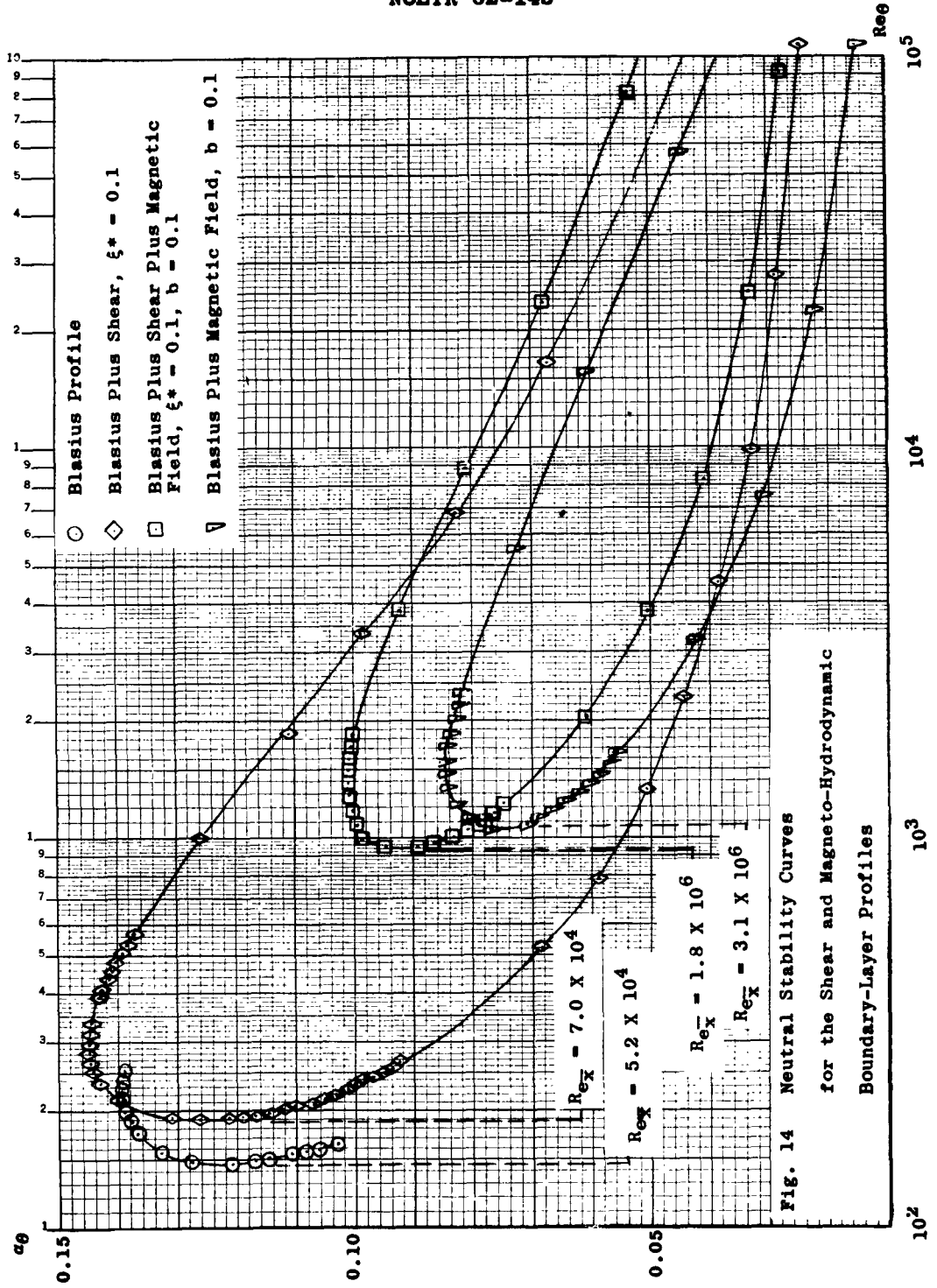
APPENDIX A*

On the "Dunn-Lin" Factor in the Secular Equation for Laminar Stability of Boundary Layers

by

S. F. Shen

Although calculations in the present report are carried out using the simplified Lees-Lin secular equation, it appears desirable to express the "Dunn-Lin" factor Δ in equation (93) of reference (1) in a more explicit manner in terms of the given flow parameters. Recent works of Mack, reference (13), and Reshotko, reference (7), suggested that further correction should be added to the original Dunn-Lin factor. By closer examination it appears that in the mass transfer case, as well as for the single-component compressible boundary layer, logically the original Dunn-Lin factor is the one to use as long as no perturbation terms of higher order than $(\alpha R_\delta)^{-1/2}$ are included in the differential equations. Partial refinement such as those of Mack or Reshotko may have the practical advantage of yielding more realistic results, but they must not be taken as consistent theories.

A few misprints and errors of NAVORD Report 4467, reference (1), meanwhile have been discovered. These are listed in the following:

Equation (3) should read:

$$\frac{\partial \rho'}{\partial t} + \bar{u}\,\frac{\partial \rho'}{\partial x} + v'\frac{d\bar{\rho}}{dy} = -\bar{\rho}\left(\frac{\partial u'}{\partial x} + \frac{\partial v'}{\partial y}\right)$$

*In this Appendix the symbols of reference (1) are used. Differences from those used in the main body of the present report are noted as the following:

Appendix:

$$Z_1 \quad Z_2 \quad Z_3 \quad Z_4 \quad Z_5 \quad Z_6 \quad Z_7 \quad Z_8 \quad W \quad \sigma \quad \phi \quad f \quad \tilde{\theta} \quad \breve{\xi} \quad c_1$$

Body of Report:

$$f_v \quad f_v' \quad \phi_v\frac{\pi_v}{M_\infty^2} \quad \theta_v \quad \theta_v' \quad \xi_v \quad \xi_v' \quad u \quad P_r \quad \phi_i \quad f_i \quad \theta_i \quad \xi_i \quad w_1$$

Equations (31) and (32) should read:

$$\frac{dZ_3}{dy} = -iZ_1 - \frac{\rho_1'}{\rho_1} Z_3 - i(w-c)\left[M_\infty^2 Z_4 - \frac{Z_5}{h_1} - \frac{Z_7}{F} \right]$$

$$\frac{dZ_4}{dy} = \left\{ 1 + \frac{\gamma\mu_1\alpha}{R_\delta} i(w-c)M_\infty^2 \right\}\left\{ -i\rho_1\alpha^2\gamma(w-c)Z_3 + \frac{\gamma\mu_1\alpha}{R_\delta}\left[i\left(\frac{\rho_1'}{\rho_1}\right)Z_1 \right. \right.$$

$$-iZ_2 - \rho_1\left(\frac{\rho_1'}{\rho_1^2}\right)'Z_3 + i\rho_1\left(\frac{w-c}{\rho_1}\right)'M_\infty^2 Z_4 + i\rho_1\left(\frac{w-c}{\rho_1 h_1}\right)'Z_5 + \frac{i(w-c)}{h_1}Z_6$$

$$\left. \left. + i\rho_1\left(\frac{w-c}{\rho_1 F}\right)'Z_7 + \frac{i(w-c)}{F}Z_8 \right]\right\} \tag{A1}$$

Equation (89) should read

$$Z_{1,3,4,5,7} \simeq \left(0,0,0,\vartheta,1\right)\exp\left\{ \sqrt{\alpha R_\delta}\int_{Y_c}^y g_3\, dy \right\}$$

$$Z_{2,6,8} \simeq \sqrt{\alpha R_v}\left(0, g_3\vartheta, g_3\right)\exp\left\{ \sqrt{\alpha R_\delta}\int_{Y_c}^y g_3\, dy \right\}$$

$$\vartheta = \left(c_{p_d} - c_{p_a}\right)\Big/ \bar{c}_p \tag{A2}$$

The right-hand side of equation (91) should read:

$$O \begin{pmatrix} 1 & \varepsilon' & \varepsilon' & \varepsilon' \\ \varepsilon' & \varepsilon' & 1 & \varepsilon' \\ \varepsilon' & \varepsilon' & 1 & 1 \\ 1 & 1 & 1 & 1 \end{pmatrix}$$

Equation (93) should read:

$$\frac{\widehat{\phi}(0)}{\widehat{f}(0)} = \frac{\phi^{(i)}(0)}{f^{(i)}(0)}\left(1+\Delta\right) \tag{A3}$$

Equation (94) should read:

$$\Delta = \frac{\phi^{(5)}(0)}{\phi^{(i)}(0)}\frac{f^{(i)}(0)}{\widehat{f}(0)}\left[\frac{\widehat{\theta}(0)}{\theta^{(5)}(0)} + \frac{\widehat{\xi}(0)}{\xi^{(7)}(0)}\left(\frac{\phi^{(7)}(0)}{\phi^{(5)}(0)} - \frac{\theta^{(7)}(0)}{\theta^{(5)}(0)}\right)\right] + O\left(\sqrt{\alpha R_\delta}\right) \tag{A4}$$

We now proceed with the evaluation of Δ. One needs first the ratios $\widehat{\theta}(0)/\widehat{f}(0)$ and $\widehat{\xi}(0)/\widehat{f}(0)$ from the inviscid solutions. By going back to equation (17) of reference (1), there results

$$\frac{\widehat{\theta}(0)}{\widehat{f}(0)} = M_c^2(\gamma-1) + i\left[M^2(\gamma-1)w'(0) - \frac{h_1'(0)}{C}\right]\frac{\widehat{\phi}(0)}{\widehat{f}(0)} \tag{A5}$$

and from equation (21) of reference (1)

$$\frac{\widehat{\xi}(0)}{\widehat{\phi}(0)} = -i\frac{C_1'(0)}{C} \tag{A6}$$

Substitution of equations (A5) and (A6) in equation (A4) and insertion of the result into equation (A3) finally lead to an explicit expression for Δ in terms of the given parameters and the viscous solutions:

$$\Delta = \left(\Delta_D + i\Delta'\right)\Big/\left(1 - i\Delta'\right) \tag{A7}$$

where: $$\Delta_D = M^2(\gamma-1)C\frac{f^{(i)}(0)}{\phi^{(i)}(0)}\frac{\phi^{(5)}(0)}{\theta^{(5)}(0)}$$

$$\Delta' = \frac{\phi^{(5)}(0)}{\theta^{(5)}(0)}\left[M^2(\gamma-1)w'(0) - \frac{h_1'(0)}{C} + \frac{C_1'(0)}{C}\frac{\theta^{(7)}(0)}{\xi^{(7)}(0)}\left(1 - \frac{\phi^{(i)}(0)}{\phi^{(5)}(0)}\frac{\theta^{(5)}(0)}{\theta^{(7)}(0)}\right)\right] \tag{A8}$$

A-3

We note that Δ_D is the original "Dunn-Lin" factor for compressible boundary layers, reference (6). The Δ'-term for the same case (compressible boundary layer without mass transfer) was regarded as further corrections by both Mack and Reshotko. With mass transfer there is now an extra term proportional to the concentration gradient at wall $(c_1'(0))$ to be added to the Δ'-term, but no effect on Δ_D.

However, from equation (87) of reference (1), it is clear that

$$\Delta_D \sim O(1)$$

$$\phi^{(5)}(0)/\theta^{(5)}(0) \sim O\left(1/\sqrt{\alpha R_\delta}\right)$$

To arrive at equation (A4), we have already omitted terms of higher order than $1/\sqrt{\alpha R_\delta}$. Thus the Δ'-term logically should also be neglected for consistency.

To illustrate that the asymptotic expansions, equations (73) to (75) of reference (1), provide the correct estimate for the viscous solutions at the wall, we next evaluate explicitly the Dunn-Lin factor on this basis. To do so the equations for the first order approximations $f_i^{(1)}$, $i = 1, 2, 3....8$ are required. These turn out to be:

$$g f_1^{(1)} + f_1^{(0)'} = f_2^{(1)} \tag{A9}$$

$$g f_2^{(1)} + f_2^{(0)'} = \frac{i}{v_1}(w-c) f_1^{(1)} + \frac{w'}{v_1} f_3^{(1)} + \frac{i}{\gamma u_1} f_4^{(1)} \tag{A10}$$

$$g f_3^{(1)} + f_3^{(0)'} = -i f_1^{(0)} - \frac{\rho_1'}{\rho_1} f_3^{(0)} + i(w-c)\left[M_\infty^2 f_4^{(0)} - \frac{f_5^{(0)}}{h_1} - \frac{f_7^{(0)}}{F} \right] \tag{A11}$$

$$g f_4^{(1)} + f_4^{(0)'} = i\alpha^2 \gamma (w-c) \rho_1 f_3^{(0)} \tag{A12}$$

A-4

$$g f_5^{(1)} + f_5^{(0)} = f_6^{(1)} \tag{A13}$$

$$g f_6^{(1)} + f_6^{(0)'} = \frac{1}{\mu_1}\left\{ [\cdots] f_3^{(1)} + [\cdots] f_4^{(1)} + i\sigma\rho_1(w-c) f_5^{(1)} + [\cdots] f_7^{(1)} \right\} \tag{A14}$$

$$g f_7^{(1)} + f_7^{(0)'} = f_8^{(1)} \tag{A15}$$

$$g f_8^{(1)} + f_8^{(0)'} = \frac{\varpi}{\nu_1} i(w-c) f_7^{(1)} + \frac{\varpi}{\mu_1} \rho_1 c_1' f_3^{(1)} \tag{A16}$$

The above equations are parallel to equations (76) to (83) of reference (1).* Again we have not written out all terms in equation (A14) for simplicity. Based upon these equations, it is found:

$$\frac{\phi^{(5)}(0)}{\theta^{(5)}(0)} = \left.\frac{f_3(0)}{f_5(0)}\right|_{g=g_2} = \frac{1}{\sqrt{\alpha R_6}} \left.\frac{f_3^{(1)}(0)}{f_5^{(0)}(0)}\right|_{g=g_2} = \frac{1}{\sqrt{\alpha R_6}} \frac{-ic}{h_1(0)} \frac{1}{g_2(0)}$$

*We should remark that in equations (85), (87) and (89) of reference (1), the expressions for Z_i represent essentially only orders of magnitude. For example, for $g = g_1$, $f_1^{(0)}$ is actually not unity but a function of y to be found from equations (A9) to (A12) here.

by using equation (A11). Similarly,

$$\frac{f^{(1)}(0)}{\phi^{(1)}(0)} = \left.\frac{f_1(0)}{f_3(0)}\right|_{g=g_1} = \sqrt{\propto R_6}\; i\, g_1(0)$$

also by using (A11). Consequently, these estimates give

$$\Delta_D = M^2(\gamma-1)\, c\; i\, g_1(0)\left(\frac{-i\, c}{h_1(0)\, g_2(0)}\right) = M^2(\gamma-1)\, c^2\!\big/\!\sqrt{\sigma}\; h_1(0) \quad \text{(A16)}$$

Comparison shows that equation (A16) of this Appendix agrees with (A.16) of Dunn and Lin's paper except for a function, "$\chi(z,\sigma)$," in the latter which is $O(1)$. (Dunn and Lin's function, $\chi(z,\sigma)$, is the ratio of Mack's $G(z_0)$ and $F(z)$ defined by equations (5-18) and (5-14), respectively, of reference (13) and tabulated as Table I therein.) From Mack's Table, for large z (say, above 6 or 7) Dunn and Lin's $\chi(z,\sigma)$ is indeed nearly unity, bearing out the validity of the asymptotic expansions.

There is no difficulty to work out the Δ'-term for the mass transfer case in a similar manner by using equation (A9) through (A15) if desired. The final result serves no useful purpose at the moment, since its order of magnitude can already be assessed as $O(1/\sqrt{\alpha R_\delta})$. In this light, both Mack's and Reshotko's "improvement" of using the Δ'-term must be regarded as theoretically inconsistent with their perturbation equations which are obtained from the complete linearized equations by keeping various terms, but none higher than $O(1/\sqrt{\alpha R_\delta})$. It may be noted that a strictly consistent theory to include up to $O(1/\alpha R_\delta)$ must also include the $\bar{v}$-component of the basic boundary layer flow.

AERODYNAMICS DEPARTMENT
EXTERNAL DISTRIBUTION LIST (A1)

	No. of Copies
Chief, Bureau of Naval Weapons Department of the Navy Washington 25, D. C.	
Attn: DLI-30	1
Attn: R-14	1
Attn: RRRE-4	1
Attn: RMGA-413	1
Office of Naval Research Room 2709, T-3 Washington 25, D. C.	
Attn: Head, Mechanics Branch	1
Director, David Taylor Model Basin Aerodynamics Laboratory Washington 7, D. C.	
Attn: Library	1
Commander, U. S. Naval Ordnance Test Station China Lake, California	
Attn: Technical Library	1
Attn: Code 503	1
Attn: Code 406	1
Director, Naval Research Laboratory Washington 25, D. C.	
Attn: Code 2027	1
Commanding Officer Office of Naval Research Branch Office Box 39, Navy 100 Fleet Post Office New York, New York	1
NASA High Speed Flight Station Box 273 Edwards Air Force Base, California	
Attn: W. C. Williams	1
NASA Ames Research Center Moffett Field, California	
Attn: Librarian	1

AERODYNAMICS DEPARTMENT
EXTERNAL DISTRIBUTION LIST (A1)

	No. of Copies
NASA	
Langley Research Center	
Langley Field, Virginia	
Attn: Librarian	3
Attn: C. H. McLellan	1
Attn: J. J. Stack	1
Attn: Adolf Busemann	1
Attn: Comp. Res. Div.	1
Attn: Theoretical Aerodynamics Division	1
NASA	
Lewis Research Center	
21000 Brookpark Road	
Cleveland 11, Ohio	
Attn: Librarian	1
Attn: Chief, Propulsion Aerodynamics Div.	1
NASA	
1520 H Street, N. W.	
Washington 25, D. C.	
Attn: Chief, Division of Research Information	1
Attn: Dr. H. H. Kurzweg, Asst. Director of Research	1
Office of the Assistant Secretary of Defense (R&D)	
Room 3E1065, The Pentagon	
Washington 25, D. C.	
Attn: Technical Library	1
Research and Development Board	
Room 3D1041, The Pentagon	
Washington 25, D. C.	
Attn: Library	1
ASTIA	10
Arlington Hall Station	
Arlington 12, Virginia	
Commander, Pacific Missile Range	
Point Mugu, California	
Attn: Technical Library	1
Commanding General	
Aberdeen Proving Ground, Maryland	
Attn: Technical Information Branch	1
Attn: Ballistic Research Laboratory	1

AERODYNAMICS DEPARTMENT
EXTERNAL DISTRIBUTION LIST (A1)

	No. of Copies
Commander, Naval Weapons Laboratory Dahlgren, Virginia Attn: Library	1
Director, Special Projects Department of the Navy Washington 25, D. C. Attn: SP-2722	1
Director of Intelligence Headquarters, USAF Washington 25, D. C. Attn: AFOIN-3B	1

Headquarters - Aero. Systems Division
Wright-Patterson Air Force Base
Dayton, Ohio
  Attn: WWAD
  Attn: RRLA-Library
	2
	1

Commander Air Force Ballistic Missile Division HQ Air Research & Development Command P. O. Box 262 Inglewood, California Attn: WDTLAR	1
Chief, Defense Atomic Support Agency Washington 25, D. C. Attn: Document Library	1

Headquarters, Arnold Engineering Development Center
Air Research and Development Center
Arnold Air Force Station, Tennessee
  Attn: Technical Library
  Attn: AEOR
  Attn: AEOIM
	1
	1
	1

Commanding Officer, DOFL Washington 25, D. C. Attn: Library, Room 211, Bldg. 92	1

Commanding General
Redstone Arsenal
Huntsville, Alabama
  Attn: Mr. N. Shapiro (ORDDW-MRF)
  Attn: Technical Library
	1
	1

AERODYNAMICS DEPARTMENT
EXTERNAL DISTRIBUTION LIST (A1)

	No. of Copies
NASA George C. Marshall Space Flight Center Huntsville, Alabama	
Attn: Dr. E. Geissler	1
Attn: Mr. T. Reed	1
Attn: Mr. H. Paul	1
Attn: Mr. W. Dahm	1
Attn: Mr. D. Burrows	1
Attn: Mr. J. Kingsbury	1
Attn: ORDAB-DA	1
APL/JHU (C/NOw 7386) 8621 Georgia Avenue Silver Spring, Maryland	
Attn: Technical Reports Group	2
Attn: Mr. D. Fox	1
Attn: Dr. F. Hill	1
Via: INSORD	
Air Force Systems Command Scientific & Technical Liaison Office Room 2305, Munitions Building Department of the Navy Washington 25, D. C.	
Attn: E. G. Haas	1

AERODYNAMICS DEPARTMENT
EXTERNAL DISTRIBUTION LIST (A2)

	No. of Copies
University of Minnesota Minneapolis 14, Minnesota	
Attn: Dr. E. R. G. Eckert	1
Attn: Heat Transfer Laboratory	1
Attn: Technical Library	1
Rensselaer Polytechnic Institute Troy, New York	
Attn: Dept. of Aeronautical Engineering	1
Dr. James P. Hartnett Department of Mechanical Engineering University of Delaware Newark, Delaware	1
Princeton University James Forrestal Research Center Gas Dynamics Laboratory Princeton, New Jersey	
Attn: Prof. S. Bogdonoff	1
Attn: Dept. of Aeronautical Engineering Library	1
Defense Research Laboratory The University of Texas P. O. Box 8029 Austin 12, Texas	
Attn: Assistant Director	1
Ohio State University Columbus 10, Ohio	
Attn: Security Officer	1
Attn: Aerodynamics Laboratory	1
Attn: Dr. J. Lee	1
Attn: Chairman, Dept. of Aero. Engineering	1
California Institute of Technology Pasadena, California	
Attn: Guggenheim Aero. Laboratory, Aeronautics Library	1
Attn: Jet Propulsion Laboratory	1
Attn: Dr. H. Liepmann	1
Attn: Dr. L. Lees	1
Attn: Dr. D. Coles	1
Attn: Mr. A. Roshko	1
Attn: Dr. J. Laufer	1
Case Institute of Technology Cleveland 6, Ohio	
Attn: G. Kuerti	1

AERODYNAMICS DEPARTMENT
EXTERNAL DISTRIBUTION LIST (A2)

	No. of Copies

North American Aviation, Inc.
Aerophysics Laboratory
Downing, California
  Attn: Dr. E. R. Van Driest — 1
  Attn: Missile Division (Library) — 1

Department of Mechanical Engineering
Yale University
400 Temple Street
New Haven 10, Connecticut
  Attn: Dr. P. P. Wegener — 1
  Attn: Prof. N. A. Hall — 1

MIT Lincoln Laboratory — 1
Lexington, Massachusetts

RAND Corporation
1700 Main Street
Santa Monica, California
  Attn: Library, USAF Project RAND — 1
  Attn: Technical Communications — 1

Mr. J. Lukasiewicz — 1
Chief, Gas Dynamics Facility
ARO, Incorporated
Tullahoma, Tennessee

Massachusetts Institute of Technology
Cambridge 39, Massachusetts
  Attn: Prof. J. Kaye — 1
  Attn: Prof. M. Finston — 1
  Attn: Mr. J. Baron — 1
  Attn: Prof. A. H. Shapiro — 1
  Attn: Naval Supersonic Laboratory — 1
  Attn: Aero. Engineering Library — 1

Polytechnic Institute of Brooklyn
527 Atlantic Avenue
Freeport, New York
  Attn: Dr. A. Ferri — 1
  Attn: Dr. M. Bloom — 1
  Attn: Dr. P. Libby — 1
  Attn: Aerodynamics Laboratory — 1

Brown University
Division of Engineering
Providence, Rhode Island
  Attn: Prof. R. Probstein — 1
  Attn: Prof. C. Lin — 1
  Attn: Librarian — 1

2

AERODYNAMICS DEPARTMENT
EXTERNAL DISTRIBUTION LIST (A2)

	No. of Copies
Air Ballistics Laboratory Army Ballistic Missile Agency Huntsville, Alabama	1
Applied Mechanics Reviews Southwest Research Institute 8500 Culebra Road San Antonio 6, Texas	1
BuWeps Representative Aerojet-General Corporation 6352 N. Irwindale Avenue Azusa, California	1

Boeing Airplane Company
Seattle, Washington
  Attn: J. H. Russell
  Attn: Research Library
	
	1
	1

United Aircraft Corporation
400 Main Street
East Hartford 8, Connecticut
  Attn: Chief Librarian
  Attn: Mr. W. Kuhrt, Research Dept.
  Attn: Mr. J. G. Lee
	
	1
	2
	1

Hughes Aircraft Company
Florence Avenue at Teale Streets
Culver City, California
  Attn: Mr. D. J. Johnson
        R&D Technical Library
	
	1

McDonnell Aircraft Corporation P. O. Box 516 St. Louis 3, Missouri	1

Lockheed Missiles and Space Company
P. O. Box 504
Sunnyvale, California
  Attn: Dr. L. H. Wilson
  Attn: Mr. M. Tucker
  Attn: Mr. R. Smelt
	
	1
	1
	1

The Martin Company
Baltimore 3, Maryland
  Attn: Library
  Attn: Chief Aerodynamicist
	
	1
	1

AERODYNAMICS DEPARTMENT
EXTERNAL DISTRIBUTION LIST (A2)

	No. of Copies
CONVAIR A Division of General Dynamics Corporation Fort Worth, Texas	
Attn: Library	1
Attn: Theoretical Aerodynamics Group	1
Purdue University School of Aeronautical & Engineering Sciences LaFayette, Indiana	
Attn: R. L. Taggart, Library	1
University of Maryland College Park, Maryland	
Attn: Director	2
Attn: Dr. J. Burgers	1
Attn: Librarian, Engr. & Physical Sciences	1
Attn: Librarian, Institute for Fluid Dynamics and Applied Mathematics	1
University of Michigan Ann Arbor, Michigan	
Attn: Dr. A. Kuethe	1
Attn: Dr. O. Laporte	1
Attn: Department of Aeronautical Engineering	1
Stanford University Palo Alto, California	
Attn: Applied Mathematics & Statistics Lab.	1
Attn: Prof. D. Bershader, Dept. of Aero. Engr.	1
Cornell University Graduate School of Aeronautical Engineering Ithaca, New York	
Attn: Prof. W. R. Sears	1
The Johns Hopkins University Charles and 34th Streets Baltimore, Maryland	
Attn: Dr. F. H. Clauser	1
Attn: Dr. M. Morkovin	1
University of California Berkeley 4, California	
Attn: G. Maslach	1
Attn: Dr. S. Schaaf	1
Attn: Dr. Holt	1
Attn: Institute of Engineering Research	1

AERODYNAMICS DEPARTMENT
EXTERNAL DISTRIBUTION LIST (A2)

	No. of Copies
Cornell Aeronautical Laboratory, Inc. 4455 Genesee Street Buffalo 21, New York	
Attn: Librarian	1
Attn: Dr. Franklin Moore	1
Attn: Dr. J. G. Hall	1
University of Minnesota Rosemount Research Laboratories Rosemount, Minnesota	
Attn: Technical Library	1
Director, Air University Library Maxwell Air Force Base, Alabama	1
Douglas Aircraft Company, Inc. Santa Monica Division 3000 Ocean Park Boulevard Santa Monica California	
Attn: Chief Missiles Engineer	1
Attn: Aerodynamics Section	1
General Motors Corporation Defense Systems Division Santa Barbara, California	
Attn: Dr. A. C. Charters	1
CONVAIR A Division of General Dynamics Corporation Daingerfield, Texas	1
CONVAIR Scientific Research Laboratory 5001 Kearney Villa Road San Diego 11, California	
Attn: Mr. M. Sibulkin	1
Attn: Asst. to the Director of Scientific Research	1
Attn: Dr. B. M. Leadon	1
Attn: Library	1
Republic Aviation Corporation Farmingdale, New York	
Attn: Technical Library	1
General Applied Science Laboratories, Inc. Merrick and Stewart Avenues Westbury, L. I., New York	
Attn: Mr. Walter Daskin	1
Attn: Mr. R. W. Byrne	1

5

AERODYNAMICS DEPARTMENT
EXTERNAL DISTRIBUTION LIST (A2)

No. of
Copies

Arnold Research Organization, Inc.
Tullahoma, Tennessee
  Attn: Technical Library   1
  Attn: Chief, Propulsion Wind Tunnel 1
  Attn: Dr. J. L. Potter   1

General Electric Company
Missile and Space Vehicle Department
3198 Chestnut Street
Philadelphia, Pennsylvania
  Attn: Larry Chasen, Mgr. Library   2
  Attn: Mr. R. Kirby   1
  Attn: Dr. J. Farber   1
  Attn: Dr. G. Sutton   1
  Attn: Dr. J. D. Stewart   1
  Attn: Dr. S. M. Scala   1
  Attn: Dr. H. Lew   1
  Attn: Mr. Jerome Persh   1
Eastman Kodak Company
Navy Ordnance Division
50 West Main Street
Rochester 14, New York
  Attn: W. B. Forman   2

Library   3
AVCO-Everett Research Laboratory
2385 Revere Beach Parkway
Everett 49, Massachusetts

AVCO-Everett Research Laboratory
201 Lowell Street
Wilmington, Massachusetts
  Attn: Mr. F. R. Riddell   1

AER, Incorporated   1
158 North Hill Avenue
Pasadena, California

Armour Research Foundation
10 West 35th Street
Chicago 16, Illinois
  Attn: Dept. M   2
  Attn: Dr. Paul T. Torda   1

Chance-Vought Aircraft, Inc.
Dallas, Texas
  Attn: Librarian   2

AERODYNAMICS DEPARTMENT
EXTERNAL DISTRIBUTION LIST (A2)

No. of
Copies

National Science Foundation
1951 Constitution Avenue, N. W.
Washington 25, D. C.
  Attn: Engineering Sciences Division   1

New York University
University Heights
New York 53, New York
  Attn: Department of Aeronautical Engineering   1

New York University
25 Waverly Place
New York 3, New York
  Attn: Library, Institute of Math. Sciences   1

NORAIR
A Division of Northrop Corp.
Hawthorne, California
  Attn: Library   1

Northrop Aircraft, Inc.
Hawthorne, California
  Attn: Library   1

Gas Dynamics Laboratory
Technological Institute
Northwestern University
Evanston, Illinois
  Attn: Library   1

Pennsylvania State University
University Park, Pennsylvania
  Attn: Library, Dept. of Aero. Engineering   1

The Ramo-Wooldridge Corporation   1
8820 Bellanca Avenue
Los Angeles 45, California

Gifts and Exchanges   1
Fondren Library
Rice Institute
P. O. Box 1892
Houston 1, Texas

University of Southern California
Engineering Center
Los Angeles 7, California
  Attn: Librarian   1

7

AERODYNAMICS DEPARTMENT
EXTERNAL DISTRIBUTION LIST (A2)

	No. of Copies
Commander Air Force Flight Test Center Edwards Air Force Base Muroc, California Attn: FTOTL	1
Air Force Office of Scientific Research Holloman Air Force Base Alamogordo, New Mexico Attn: SRLTL	1
The Editor Battelle Technical Review Battelle Memorial Institute 505 King Avenue Columbus 1, Ohio	1
Douglas Aircraft Company, Inc. El Segundo Division El Segundo, California	1
Fluidyne Engineering Corp. 5740 Wayzata Blvd. Golden Valley Minneapolis 16, Minnesota	1
Grumman Aircraft Engineering Corp. Bethpage, L. I., New York	1
Lockheed Missile and Space Company P. O. Box 551 Burbank, California Attn: Library	1
Marquardt Aircraft Corporation 7801 Havenhurst Van Nuys, California	1
The Martin Company Denver, Colorado Attn: Library	1
Mississippi State College Engineering and Industrial Research Station Aerophysics Department P. O. Box 248 State College, Mississippi	1

AERODYNAMICS DEPARTMENT
EXTERNAL DISTRIBUTION LIST (A2)

No. of
Copies

Lockheed Missile and Space Company
3251 Hanover Street
Palo Alto, California
   Attn: Mr. J. A. Laurmann   1
   Attn: Library

General Electric Company
Research Laboratory
Schenectady, New York
   Attn: Dr. H. T. Nagamatsu   1
   Attn: Library

Fluid Dynamics Laboratory
Mechanical Engineering Department
Stevens Institute of Technology
Hoboken, New Jersey
   Attn: Dr. R. H. Page, Director   1

Department of Mechanical Engineering
University of Arizona
Tucson, Arizona
   Attn: Dr. E. K. Parks   1

Vitro Laboratories
200 Pleasant Valley Way
West Orange, New Jersey
   Attn: Dr. Charles Sheer   1

Department of Aeronautical Engineering
University of Washington
Seattle 5, Washington
   Attn: Prof. R. E. Street   1
   Attn: Library   1

Aeronautical Engineering Review   1
2 East 64th Street
New York 21, New York

Institute of the Aerospace Sciences
2 East 64th Street
New York 21, New York
   Attn: Managing Editor   1
   Attn: Library   1

Department of Aeronautics   1
United States Air Force Academy
Colorado

AERODYNAMICS DEPARTMENT
EXTERNAL DISTRIBUTION LIST (A2)

No. of
Copies

MHD Research, Inc.
Newport Beach, California
  Attn: Dr. V. H. Blackman, Technical Director   1

University of Alabama
College of Engineering
University, Alabama
  Attn: Prof. C. H. Bryan, Head
        Dept. of Aeronautical Engineering   1

Office of Naval Research
Bldg. T-3, Department of the Navy
17th and Constitution Avenue
Washington 25, D. C.
  Attn: Mr. Ralph D. Cooper, Head
        Fluid Dynamics Branch   1

ARDE Associates
100 W. Century Road
Paramus, New Jersey
  Attn: Mr. Edward Cooperman   1

Aeronautical Research Associates of Princeton
50 Washington Road
Princeton, New Jersey
  Attn: Dr. C. duP. Donaldson, President   1

Daniel Guggenheim School of Aeronautics
Georgia Institute of Technology
Atlanta, Georgia
  Attn: Prof. A. L. Ducoffe   1

University of Cincinnati
Cincinnati, Ohio
  Attn: Prof. R. P. Harrington, Head
        Dept. of Aeronautical Engineering   1

Virginia Polytechnic Institute
Dept. of Aerospace Engineering
Blacksburg, Virginia
  Attn: Mr. R. T. Keefe   1
  Attn: Library   1

IBM Federal System Division
7220 Wisconsin Avenue
Bethesda, Maryland
  Attn: Dr. I. Korobkin   1

10

AERODYNAMICS DEPARTMENT
EXTERNAL DISTRIBUTION LIST (A2)

No. of
Copies

Superintendent
U. S. Naval Postgraduate School
Monterey, California
  Attn: Technical Reports Section Library   1

National Bureau of Standards
Washington 25, D. C.
  Attn: Chief, Fluid Mechanics Section   1

North Carolina State College
Raleigh, North Carolina
  Attn: Prof. R. W. Truitt, Head
        Dept. of Mechanical Engineering   1
  Attn: Division of Engineering Research
        Technical Library   1

Apollo - DDCS
General Electric Company
A&E Bldg., Rm. 204
Daytona Beach, Florida
  Attn: Dave Hovis   1

CATALOGING INFORMATION FOR LIBRARY USE

BIBLIOGRAPHIC INFORMATION

	DESCRIPTORS	CODES	DESCRIPTORS	CODES
SOURCE	NOL technical report	NOLTR	Unclassified - 28	U028
REPORT NUMBER	62-143	620143		
REPORT DATE	13 March 1963	0363		

SECURITY CLASSIFICATION AND CODE COUNT
CIRCULATION LIMITATION
CIRCULATION LIMITATION OR BIBLIOGRAPHIC
BIBLIOGRAPHIC (SUPPL., VOL., ETC.)

SUBJECT ANALYSIS OF REPORT

DESCRIPTORS	CODES	DESCRIPTORS	CODES	DESCRIPTORS	CODES
Stability	STBI	Magnetohydrodynamics	MAGT	Flow	FLOW
Boundary-layer	BOUL	Solving	SOLG	Aerodynamics	AERD
Profiles	PROF	Inviscid	VISCX	Zero	0000
Gas	GASE	Viscous	VISC	Mach number	MACH
Injection	INJC	Eigenvalue	EIGV		
Magnetic fields	MAGI	Data	DATA		
External	EXTR	Transport	TANP		
Shear	SHER	Properties	PROP		
Applied	APPI	Blasius	BLSI		
Quantitative	QUAZ	Laminar	LAMI		
Linearized	LINN	Transition	TRNI		
Equations	EQUA	Turbulent	TUBU		

Naval Ordnance Laboratory, White Oak, Md.
(NOL technical report 62-143)
THE STABILITY OF SELECTED BOUNDARY-LAYER
PROFILES (U), by John O. Powers and others.
13 March 1963. v.p.; diagr. (Aerodynamics
research report 186) Task RMGA-41-034.
UNCLASSIFIED

Investigation of stability characteristics
of infinitesimal disturbances in laminar bound-
ary-layer profiles has been conducted. Re-
sults give quantitative indications of influ-
ence on boundary-layer stability of foreign
gas injection, applied magnetic fields, and
applied external shear. It is quantitatively
shown that injected gases of large molecular
weight and diameter may result in stabiliza-
tion, whereas the light small diameter gases
are generally destabilizing except for large
values of wall-to-free-stream temperature
ratio.

1. Boundary layer
   Stability
2. Boundary layer
   Flow
3. Flow, Turbulent
4. Flow fields
I. Title
II. Powers, John O.
III. Series
IV. Project

Abstract card is
unclassified.

Naval Ordnance Laboratory, White Oak, Md.
(NOL technical report 62-143)
THE STABILITY OF SELECTED BOUNDARY-LAYER
PROFILES (U), by John O. Powers and others.
13 March 1963. v.p.; diagr. (Aerodynamics
research report 186) Task RMGA-41-034.
UNCLASSIFIED

Investigation of stability characteristics
of infinitesimal disturbances in laminar bound-
ary-layer profiles has been conducted. Re-
sults give quantitative indications of influ-
ence on boundary-layer stability of foreign
gas injection, applied magnetic fields, and
applied external shear. It is quantitatively
shown that injected gases of large molecular
weight and diameter may result in stabiliza-
tion, whereas the light small diameter gases
are generally destabilizing except for large
values of wall-to-free-stream temperature
ratio.

1. Boundary layer
   Stability
2. Boundary layer
   Flow
3. Flow, Turbulent
4. Flow fields
I. Title
II. Powers, John O.
III. Series
IV. Project

Abstract card is
unclassified.

Naval Ordnance Laboratory, White Oak, Md.
(NOL technical report 62-143)
THE STABILITY OF SELECTED BOUNDARY-LAYER
PROFILES (U), by John O. Powers and others.
13 March 1963. v.p.; diagr. (Aerodynamics
research report 186) Task RMGA-41-034.
UNCLASSIFIED

Investigation of stability characteristics
of infinitesimal disturbances in laminar bound-
ary-layer profiles has been conducted. Re-
sults give quantitative indications of influ-
ence on boundary-layer stability of foreign
gas injection, applied magnetic fields, and
applied external shear. It is quantitatively
shown that injected gases of large molecular
weight and diameter may result in stabiliza-
tion, whereas the light small diameter gases
are generally destabilizing except for large
values of wall-to-free-stream temperature
ratio.

1. Boundary layer
   Stability
2. Boundary layer
   Flow
3. Flow, Turbulent
4. Flow fields
I. Title
II. Powers, John O.
III. Series
IV. Project

Abstract card is
unclassified.

Naval Ordnance Laboratory, White Oak, Md.
(NOL technical report 62-143)
THE STABILITY OF SELECTED BOUNDARY-LAYER
PROFILES (U), by John O. Powers and others.
13 March 1963. v.p.; diagr. (Aerodynamics
research report 186) Task RMGA-41-034.
UNCLASSIFIED

Investigation of stability characteristics
of infinitesimal disturbances in laminar bound-
ary-layer profiles has been conducted. Re-
sults give quantitative indications of influ-
ence on boundary-layer stability of foreign
gas injection, applied magnetic fields, and
applied external shear. It is quantitatively
shown that injected gases of large molecular
weight and diameter may result in stabiliza-
tion, whereas the light small diameter gases
are generally destabilizing except for large
values of wall-to-free-stream temperature
ratio.

1 Boundary layer
   Stability
2. Boundary layer
   Flow
3. Flow, Turbulent
4. Flow fields
I. Title
II. Powers, John O.
III. Series
IV. Project

Abstract card is
unclassified.